Water Resources Research

RESEARCH ARTICLE
10.1029/2024WR037086

The Role of Lithology on Concentration-Discharge Relationships and Carbon Export in Two Adjacent Headwater Catchments

L. Giggy[1] and M. Zimmer[1,2]

[1]Department of Earth and Planetary Sciences, University of California Santa Cruz, Santa Cruz, CA, USA, [2]Department of Soil and Environmental Sciences, University of Wisconsin Madison, Madison, WI, USA

Key Points:

- Bedrock lithology drives differences in streamflow and carbon export in adjacent catchments, controlling variability in shallow flow paths
- Both catchments display similar in-stream major ion concentrations and chemostatic behavior, likely driven by rapid chemical reactions
- Individual storm events have an outsized effect on annual chemical export patterns

Supporting Information:

Supporting Information may be found in the online version of this article.

Correspondence to:

L. Giggy,
lgiggy@ucsc.edu

Citation:

Giggy, L., & Zimmer, M. (2025). The role of lithology on concentration-discharge relationships and carbon export in two adjacent headwater catchments. *Water Resources Research*, *61*, e2024WR037086. https://doi.org/10.1029/2024WR037086

Received 9 JAN 2024
Accepted 19 FEB 2025

Abstract Headwater catchments have strong impacts on downstream waterways, near-shore ecosystems, and the quality of water available for growing human populations. Thus, understanding how water and solutes are exported through these upland landscapes is critically important. A growing body of literature highlights the interaction of topography, climate, and the critical zone structure as a key control on streamflow and chemical export. However, more focused work is needed to pinpoint how variability in subsurface structure across lithologically complex regions impacts streamflow and chemical signals at catchment outlets. Here, we aim to better understand how lithology and subsurface critical zones modulate streamflow response and solute export patterns in two central coastal California headwater catchments that are similar in topography, vegetation, and climate but have different lithologies. We monitored streamflow and collected surface water samples at the catchment outlets for dissolved major ions and organic carbon (DOC) for two consecutive water years. The catchment with mélange bedrock displayed much flashier hydrologic behavior with 7.8 times higher peak flow values and 1.9 times higher mean event concentrations of DOC, suggesting shorter and shallower hydrologic flow paths that likely arise from regions of shallower bedrock. Despite distinct hydrologic behavior and DOC export, dissolved major ion concentrations were broadly similar and chemostatic, which may be driven by rapid chemical reactions in the critical zone of both catchments. Our work contributes to building an integrated understanding of how subtle differences in catchment structure can have profound impacts on how water and solutes are routed through headwater catchments.

1. Introduction

Decades of hydrologic research have aimed to build hierarchical frameworks to understand how climate and internal catchment characteristics interact to produce observed streamflow and solute export patterns in headwater catchments. While topography has been shown to be a first-order control on water routing (Beven & Kirkby, 1979; Nippgen et al., 2011; Prancevic & Kirchner, 2019), several studies have observed disparate streamflow behavior in similarly sloped landscapes (Bergstrom et al., 2016; Gutiérrez-Jurado et al., 2019). This body of work points toward soil type and bedrock lithology as additional key controls on water storage, release, and residence times in headwater catchments. Particularly, bedrock lithology and soil type set the foundation for variability in porosity and permeability of the subsurface and thus control the volume of water storage, rates of water movement, and influence the chemical signature of stream water (Han et al., 2020; Pfister et al., 2017; Tague & Grant, 2004; van Meerveld et al., 2007; Xiao et al., 2019). This prior work on streamflow generation suggests that considering the subsurface critical zone and bedrock lithology in tandem with topographic features is key to understanding observed signals at catchment outlets.

A growing body of work characterizing the subsurface critical zone shows strong links between subsurface properties and water storage and runoff. However, additional work is needed to specifically investigate links between subsurface properties and water quality, especially in lithologically complex regions. One such challenging landscape is coastal California, which contains the Franciscan complex, characterized by chaotic mixtures of rock types and complex tectonic and metamorphic histories, and underlies a large fraction of northern and central California's coastal regions (Jennings et al., 2010; Raymond, 2018, Figure 1). Drilling and long-term monitoring efforts at the Eel River Critical Zone Observatory (CZO) have characterized the critical zone in mélange bedrock associated with the Central Belt and sedimentary bedrock associated with the Coastal Belt of the Franciscan complex (Hahm et al., 2019; Rempe & Dietrich, 2018; Salve et al., 2012). This work showed that mélange hillslopes develop thin critical zones with lower saturated hydraulic conductivity, while sedimentary

hillslopes develop a deeper critical zone with higher porosity (Hahm et al., 2019). These distinctions in critical zone structure result in distinct streamflow regimes and recession rates, where catchments with a higher fraction of mélange bedrock have less summer runoff and quicker streamflow recession (Dralle et al., 2023). Similar links between upslope groundwater contributions and recession rates have been shown in numerous other catchments across the United States and Canada (Li & Ameli, 2023). This work builds a framework for the subsurface critical zone and its influence on streamflow persistence and drought vulnerability (Dralle et al., 2023; Li & Ameli, 2023; Lovill et al., 2018), water storage (Dralle et al., 2018), vegetation (Hahm et al., 2019), and salmonid habitat (Dralle et al., 2023) in regions with mixed lithologies and distinct critical zone structures. However, there is a need to extend this work toward understanding how lithologic complexity and resulting subsurface properties may influence water quality and solute export.

While a wide variety of solute export patterns have been observed in headwater catchments, there is a long-standing understanding that streamflow is composed of water with distinct chemical signals generated from distinct subsurface stores (i.e., pre-event groundwater, soil water, direct rainfall, etc.; Klaus & McDonnell, 2013; Mulholland, 1993; Sklash et al., 1976). Changes in surface water chemistry with discharge or concentration-discharge (C-Q) relationships are commonly used to examine the relative contributions from different subsurface stores of water over space and time, and leveraged for understanding the geochemical evolution of landscapes and predicting water quality parameters (Bieroza et al., 2018; Chorover et al., 2017; D'Amario et al., 2021; Holz, 2010). Depending on the solute source, geochemical reactions, and connectivity of hydrologic flow paths, solute concentrations are known to increase, decrease, or remain stable as discharge increases. During baseflow conditions, surface water is largely supported by groundwater contributions with long residence times and extended interactions with bedrock, generating streamflow with high concentrations of weathering-derived ions (major ions: Ca^{2+}, Cl^{-}, Na^{+}, Mg^{2+}, SO_4^{2-}, Si^{4+}, etc; Maher, 2011). In contrast, during periods of high rainfall, as shallow and rapid flow paths through the soil are activated, stream flow generated is expected to have higher concentrations of biogenic solutes (carbon, nitrogen, etc.), and lower major ion concentrations (Jobbágy & Jackson, 2000). As a result, major ions tend to become diluted with increasing discharge, and biogenic solutes tend to be mobilized with increasing discharge. This concept has been termed the "shallow-deep hypothesis" (Stewart et al., 2022; Zhi & Li, 2020), and while it has been shown to succinctly capture solute export patterns in some landscapes, it also suggests that catchments with distinct differences in the hydrologic flow path depths and critical zone structures should have distinct C-Q relationships. However, C-Q patterns at catchment outlets integrate processes occurring on multiple timescales (i.e., slow bedrock weathering and rapid in-stream biogeochemical processing) and are also influenced by past and present climate, vegetation, and topography, leading to differences in C-Q patterns across hydroclimatic regions and timescales (Godsey et al., 2019; Speir et al., 2024). Concentration-discharge patterns at different timescales can also yield distinct behavior driven by different processes (Knapp et al., 2020; Speir et al., 2024); thus, considering multiple timescales together can provide a more integrated understanding of catchment hydrologic and biogeochemical processes. Specifically, considering event-scale C-Q patterns is likely to be important for headwater catchments that often have punctuated and intermittent streamflow. While the critical zone has been implicated as an important control of C-Q behavior (Godsey et al., 2019), more C-Q-focused work is needed in landscapes with similar climates and topography to pinpoint the role of the lithology and subsurface critical zones on chemical signals at the catchment outlet across multiple timescales.

To address the above knowledge gaps, we instrumented two adjacent headwater catchments that are similar in climate, vegetation, and topography but have differences in bedrock, with one catchment underlain by both sedimentary and mélange lithologies and the other catchment underlain only by sedimentary lithologies. We conducted topographic analyses and monitored streamflow and solute export (Ca^{2+}, Cl^{-}, Na^{+}, Mg^{2+}, SO_4^{2-}, K^{+}, dissolved organic carbon (DOC)) from these two catchments over two consecutive water years. Here, we compare our observations with other work in these rock types to see if variability within rock types influences runoff. Further, we explore how hypothesized differences in critical zone structures from different rock types influence water quality and C-Q export patterns. Together, we aim to contribute to understanding the links between bedrock lithology, hydrologic behavior, and solute export in coastal California catchments.

2. Site Description

2.1. Blue Oak Ranch Reserve Study Site Characteristics and Wildfire

Blue Oak Ranch Reserve (BORR) is located in the Diablo Range of central California (37.3813°, −121.7367°). Within BORR, we instrumented two adjacent catchments, North Dark Canyon (NDC) and South Dark Canyon (SDC) (Figure 2). Both study catchments contain stream reaches with non-perennial flow; flow at the catchment outlets only occurs during wet winter months, primarily from October to June. NDC and SDC are 0.71 and 0.99 km^2 in size, respectively. Elevation ranges from 571 to 772 m above mean sea level (amsl) in NDC and 571–857 m amsl in SDC. Blue Oak Ranch Reserve has a Mediterranean climate with average annual air temperature measured from a weather station ∼0.6 km southeast of the catchment outlets of 13.8°C from 2011 to 2022. Air temperatures peak in summer, reaching up to 42°C, and can fall to −6°C during winter. On average, 568 mm of annual precipitation falls primarily between October to April as rain. However, this region experiences high interannual variability in precipitation totals, with regular droughts and deluges (Dettinger et al., 2011). Vegetation across both study catchments is strongly aspect-dependent, where south-facing slopes in both catchments are dominated by grasses (*Avena sp., Bromus diandrus*, and *Elymus glaucus*) with limited trees, while north-facing slopes contain blue oak and California black oak (*Quercus douglasii* and *Quercus kelloggii*). Some California bay laurel (*Umbellularia californica*) and California buckeye (*Aesculus californica*) can be found in valley bottoms (Donaldson et al., 2023).

In August 2020, both catchments were entirely burned in the Santa Clara Unit (SCU) lightning complex fire. The Monitoring Trends in Burn Severity program (MTBS; Eidenshink et al., 2007) classified the burn severity as low with small patches of moderate, calculated using the differenced Normalized Burn Ratio (dNBR). This matches our field-based determinations which indicated that the entire study area experienced a low-severity burn except at a limited number of trees, snags (dead standing trees), or woody debris that allowed for small areas of higher burn severity. We did not observe any soil hydrophobicity.

2.2. Geologic History

Bedrock geology mapping of the field site and the surrounding region has been published in several maps; however, the maps are not entirely in agreement, highlighting the geologic complexity of this region. Dibblee and Munich (2006) mapped both NDC and SDC catchment areas as Franciscan Assemblage sandstone, meta-greywacke, and containing jadeite and lawsonite. Dibblee and Munich (2006) mapped an N-S striking fault along the mainstem of NDC with "Franciscan metamorphic" rocks to the west of the fault and "Great Valley Sequence" to the east. Wentworth et al. (1999) also mapped the same fault along the mainstem of NDC but mapped "Franciscan mélange" to the west and "Yolla Bolly Terrane" to the east. Additionally, larger maps of central and northern California show the field site falls within a non-schitose blueschist facies Franciscan complex unit (Schemmann et al., 2008; Wakabayashi, 2017). The exact boundaries between units of the Franciscan complex, Yolla Bolly Terrane, and Great Valley Sequence is quite complex, much of which remains an ongoing geologic investigation evidenced by the variability in regional geologic maps of BORR.

While, determining the exact age and geologic units is outside the scope of this to clarify these various geologic reports, we conducted geologic field mapping in the summer of 2021 (Figure 1). We observed two distinct bedrock lithologies that are subsequently described as Franciscan mélange and Franciscan sedimentary. We observed metamorphic rocks, including blueschist, chert, slate, metagraywacke sandstone, and sedimentary rocks, including greywacke and shale, on the western slopes of NDC. These rock types, the presence of large blocks of more coherent, sedimentary material, and some evidence of shallow landslides are consistent with high-pressure, low-temperature metamorphism and descriptions of Franciscan mélange (Page, 1999; Raymond, 2018). The rest of the field area is underlain by steep to moderately dipping greywacke sandstone with thin interbeds of shale and occasional semi-phyllite. We describe regions underlain by these rock types as Franciscan sedimentary (Figure 1). Due to the observed differences in lithology between hillslopes, we also inferred a northeast-trending fault along the mainstem of NDC. The outlets of the study catchments sit approximately 1 km northeast of the active Calaveras fault, which accommodates 2–14 mm/yr of movement (Chaussard et al., 2015).

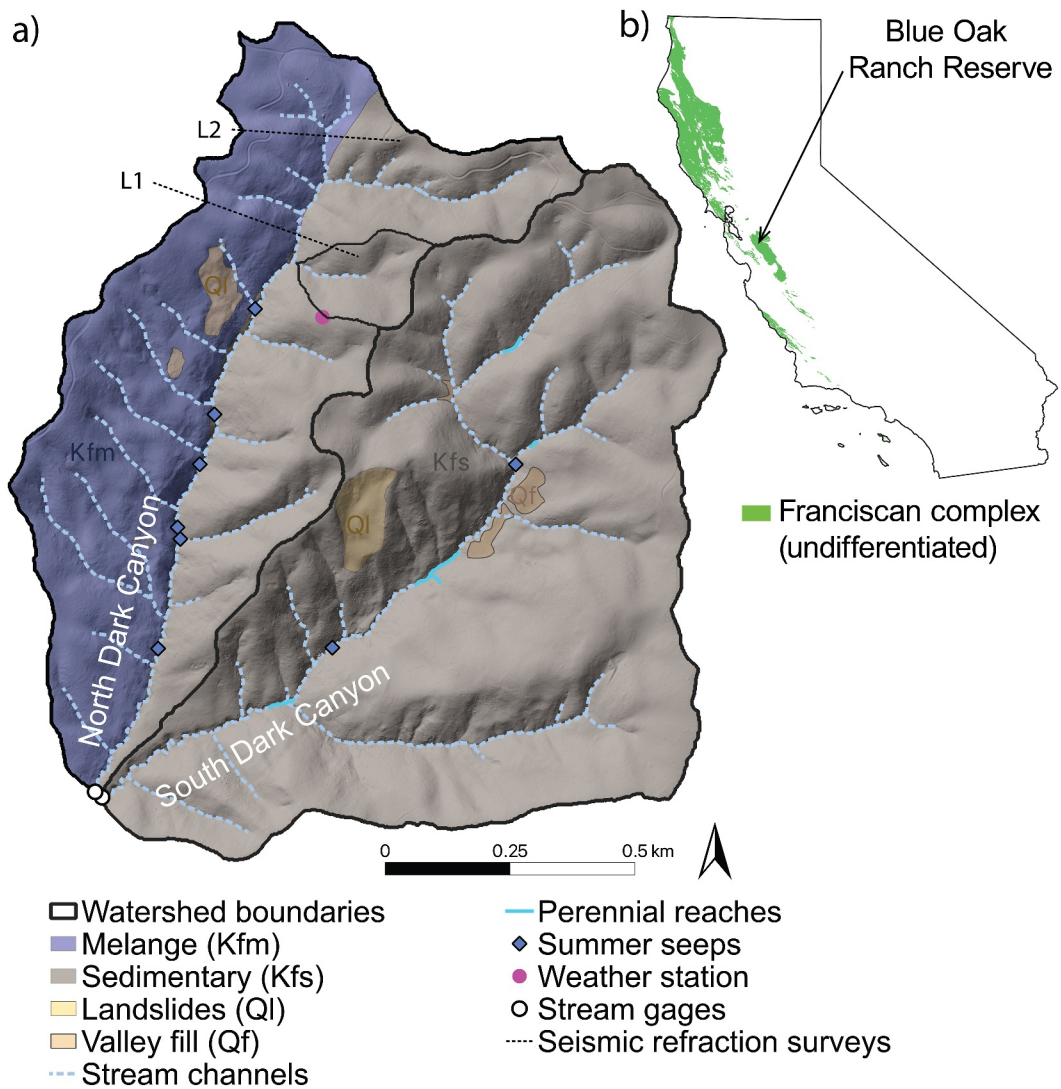

Figure 1. (a) Geologic map of the study area. Franciscan mélange geology is shown in blue, and Franciscan sedimentary in gray; small landslides and alluvial fill regions are shown in gold and tan. Approximately 50% of North Dark Canyon is underlain by mélange and 50% by sedimentary. 100% of South Dark Canyon is underlain by sedimentary. Preliminary seismic refraction survey locations are labeled L1 and L2 and shown by black dashed lines. (b) Extent of the Franciscan complex in California (Jennings et al., 2010), and the location of the field site at Blue Oak Ranch Reserve in central coastal California (37.3813°, −121.7367°).

2.3. Preliminary Geophysical Characterization of the Critical Zone

In addition to geologic mapping, preliminary critical zone characterization at BORR was done through geophysical observation of seismic velocities through two mélange-sedimentary transects (Figure 1; Figures S3 and S4 in Supporting Information S1). The mélange regions of the seismic lines showed slightly shallower depths to bedrock (19.75–25.25–2,500 m/s velocities) compared to the sedimentary regions (27.75–31.75–2,500 m/s velocities). We note that our observations differ from the Eel River CZO, which showed significant differences in bedrock depth between mélange and sedimentary rock types (Hahm et al., 2019). The geophysical observations at BORR are limited in spatial extent and do not capture the full range of rock types observed across NDC's mélange hillslopes.

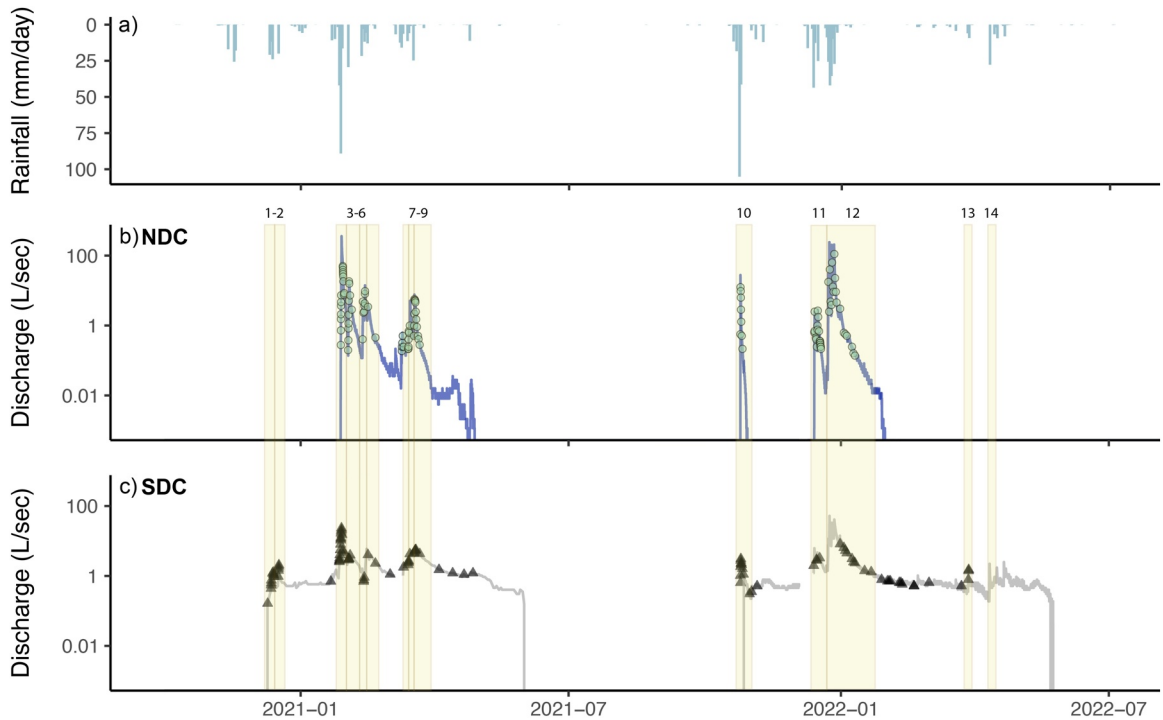

Figure 2. (a) Rainfall (mm/day), (b) North Dark Canyon (NDC) stream discharge in L/s with surface water samples from NDC denoted by light blue circles. The highest discharge observed at NDC was 359 L/s. (c) South Dark Canyon (SDC) stream discharge in L/s with surface water samples from SDC denoted by black triangles. The highest discharge observed at NDC was 52 L/s. (b, c) Light yellow boxes and numbers in panel b denote each streamflow event used to determine mean concentrations and event concentration-discharge relationships. Discharge that drops below 0.01 L/s are periods of zero flow.

3. Methods

3.1. Topographic Analyses

We conducted topographic analyses on a 30 cm resolution bare earth LiDAR collected in 2020 by Santa Clara County. We extracted stream channels in QGIS SAGA Toolbox (Conrad et al., 2015) and then adjusted them to match the channelization observed in the field (Text S1 in Supporting Information S1; Figures S1 and S2 in Supporting Information S1). Elevation, topographic slope, curvature, and drainage density were calculated in QGIS. Prior to extracting curvature values, the digital elevation model was smoothed using a 20 m radial Gaussian filter to capture hillslope scale curvature values and avoid the effects of microtopography (Prancevic & Kirchner, 2019). We binned topographic analyses and calculated mean values by catchment areas (NDC and SDC) and by underlying bedrock (mélange and sedimentary).

3.2. Stream and Climate Instrumentation

We measured discharge at the stream outlets of NDC and SDC from September 2019 to January 2023 at 5 min intervals. Here we present the data from the 2021 and 2022 water years. We developed stage-discharge rating curves at the outlets of NDC and SDC with salt dilution gaging (Day, 1976) and area-velocity techniques (Herschy, 1993). We assumed a power-law relationship between stage and discharge in the form of:

$$Q = \ell Z^{6} \quad (1)$$

Here, ℓ and 6 are constants, Z is the water height recorded at a capacitance TruTrack water height data logger (Christchurch, New Zealand) with ±1 mm resolution, and Q is stream discharge. We developed rating curves by taking point measurements of discharge across a wide range of flow conditions. We used 46 discharge measurements at NDC and 60 at SDC to determine the rating curve relationship. Stage values that exceeded the range of measured discharge at NDC had an exceedance probability of <0.18%. We did not need to extrapolate the rating curve at SDC beyond point measurements of discharge for study years presented in this manuscript.

We recorded climate data every 15 min at a weather station (ClimaVUE50, Campbell Scientific; Logan, Utah) located at a ridge top position in NDC. We assumed that rainfall totals recorded in NDC are representative of SDC due to their proximity and the limited spatial extent (~1 km^2) of the catchments. We defined precipitation events with a minimum precipitation amount of 1 mm and a minimum period without precipitation of 12 hr (Donaldson et al., 2023). For historical context of annual precipitation totals, we used a weather station managed by the Santa Clara Valley Water District (Haskin Ranch, Precipitation Sensor 6,034) located approximately 3 km northwest of the study catchment outlets with >30 years of precipitation records.

3.3. Water Sample Collection and Analysis

During storm events, we collected surface water samples at 1 to 3 hour intervals at the NDC and SDC catchment outlets using Teledyne ISCO automated water samplers (6712 and 6172C Portable Samplers). After the inflection point on the receding limbs of storm event hydrographs, we reduced sample intervals to 12 hr or daily. We collected samples by hand every 1–3 weeks during baseflow conditions. We sampled groundwater seep samples 1–2 times per year in summer months when stream channels were otherwise dry by collecting dripping water on the seep face or from small flowing pools with a syringe to reduce sediment in the samples. Precipitation samples were collected in a clearing at a ridgetop position away from tree canopies. Due to the often-limited sample volumes for precipitation, we analyzed 11 precipitation samples for all major ions and three samples for DOC during the study period.

To analyze major ions (Cl^-, Ca^{2+}, Na^+, K^+, Mg^{2+}, SO_4^{2-}), we refrigerated samples until filtered through a 0.45-micron PES filter within 48 hr of collection, then stored in a freezer until analysis. Dissolved organic carbon samples were filtered through an ashed GF/F filter, acidified with HCl to pH 2, and stored in the fridge. Major ion samples were processed at the UC Santa Cruz Marine Analytical Laboratory and Duke River Center analytical laboratory. All anions at the University of California Santa Cruz (UCSC) and all ions at Duke were measured using a Dionex ICS-2000 Ion Chromatograph. All cations at UCSC were measured using a Thermo iCap 7400 radial view Inductively Coupled Plasma Optical Emission spectrometer. Dissolved organic carbon samples were analyzed on the Shimadzu Total Organic Carbon and Nitrogen Analyzer at Rensselaer Polytechnic Institute and UCSC's Marine Analytical Laboratory.

3.4. Event Scale Analyses

We analyzed the hydrograph and stream water chemistry for trends across the entire study period (October 2020–September, 2022), each water year (2021 and 2022), and at the event scale. We use site specific information to define the start of a streamflow event as either a shift from dry to flowing conditions or the start of a precipitation event to aid in comparison between the two study catchments. While more algorithmic methods of event delineation have been proposed (Giani et al., 2022; Gnann et al., 2021), manual inspection and site-specific information can still be required (McMillan et al., 2023). Similar ad hoc metrics based on the beginning of threshold rainfall events and a specific discharge value can be found in recent literature (von Freyberg et al., 2018; Grande et al., 2022). Here, we define the end of a streamflow event at the beginning of a new precipitation event larger than 15 mm or when SDC's streamflow reaches 150% of its baseflow value (1.02 L/s). We found using a smaller value (e.g., 120% of baseflow) occasionally resulted in excessively long streamflow events at SDC. We also found smaller precipitation thresholds created excessive streamflow events that did not reflect trends observed in the hydrograph. We use SDC's baseflow value as the time cutoff for events in both catchments to aid in comparison of both catchments and due to the lack of baseflow in NDC. We determined SDC's baseflow value by taking the mean discharge during periods of flow with zero precipitation for at least 30 days prior.

We calculated each streamflow event's mean concentration (MC) using a period-weighted approach (Aulenbach et al., 2016). We linearly interpolated the concentration between samples to determine an event load, then divided by the total event streamflow (L) to determine a mean event concentration (mg/L). Event scale mean concentrations were only calculated for events with three or more samples. We collected surface water samples from 10 of the 10 streamflow events observed at NDC and 11 of the 14 streamflow events observed at SDC.

3.5. C-Q Slopes and Streamflow Recession Calculations

The relationship between stream discharge and the concentration of dissolved solutes can provide insight into the residence time of water, hydrologic flow paths, and biogeochemical processing in a catchment, enabling a

stronger understanding of how catchments store and release water. Concentration-discharge relationships tend to have a linear relationship when plotted in log-log space, indicating a power law relationship in the form of:

$$c = aQ^b \tag{2}$$

here c is the concentration of the solute, Q is discharge, and a and b are constants. This power law relationship is equivalent to:

$$\log_{10} c = \log_{10} a + b \log_{10} Q \tag{3}$$

Therefore, we can fit the concentration and discharge data set in log-log space with a least squares linear regression, where a is the y-intercept and b is the slope of the logC-logQ (here in C-Q) relationship (Hall, 1970).

We first determined the C-Q relationships at each catchment using all surface water samples collected in the 2-year study period, then separated by water year and event scale. We focus our analysis on the slope of the logC-logQ relationship, similar to Zhi and Li (2020), Stewart et al. (2022), Xiao et al. (2024) and others. Some studies define C-Q relationships based on the ratio of the coefficient of variation of concentration and the coefficient of variation of discharge (CV_c/CV_Q) or a combination of both CV_c/CV_Q and the slope of the C-Q relationship. Generally, CV_c/CV_Q values < 0.5 are considered chemostatic, and CV_c/CV_Q values > 0.5 are considered chemodynamic (Musolff et al., 2017). To aid in comparison, we make CV_c/CV_Q available in Table 2 and Tables S1 and S2 in Supporting Information S1. Here, following Godsey et al. (2009), define C-Q behavior using a slope cutoff value ±0.2. Slopes between −0.2 and +0.2 occur when the solute concentration has little variation or varies independently of discharge and are considered chemostatic. Slopes greater than +0.2 have chemodynamic flushing behavior where the solute concentration increases as discharge increases. Slopes less than −0.2 have chemodynamic dilution behavior where the solute concentration decreases as discharge increases. We excluded events with less than four samples or events with extremely limited changes in discharge (less than a 100% change between the minimum discharge sample and maximum discharge sample) from event scale C-Q analysis to avoid overfitting.

We also compare the streamflow recession of the two study catchments. We calculated rates of streamflow recession at each catchment by selecting all data points in the discharge time series that had a negative change in discharge over time (-dQ/dt), indicating periods of streamflow recession. We compared recession at the two catchments using the slope of the linear relationship between -dQ/dt and Q plotted in log-log space (Kirchner, 2009). This is a simple approach to recession that encapsulates stormflow recession and baseflow recession and does not use a threshold value for a minimum recession period. We do not use these values to determine aquifer properties, which is outside the scope of this study.

4. Results

4.1. Topography

The NDC and SDC catchments have similar catchment areas, mean topographic slopes, and mean curvatures but notably distinct drainage densities (Table 1). Catchment areas of NDC and SDC are 0.77 and 0.91 km^2, respectively. North Dark Canyon and SDC are both steep catchments with average topographic slopes of 23.6° (standard deviation (SD): 8.5) and 24.6° (SD: 8.8), respectively. The mean profile curvature of NDC is -2.77×10^{-5} 1/m (SD: 0.0015), and SDC is -4.62×10^{-5} 1/m (SD: 0.0015). The drainage densities in NDC and SDC are 7.5 km/km^2 and 5.3 km/km^2, respectively. The higher drainage density in NDC is driven by the presence of mélange. The portion of NDC underlain by mélange has a drainage density of 11.1 km/km^2, while all sedimentary regions (NDC and SDC) have a drainage density of 6.20 km/km^2. The average stream gradient of NDC is 13.4° (SD:11.4) and 13.6° (SD:11.7) at SDC. However, tributaries in NDC underlain by mélange bedrock are steeper, with an average gradient of 16.5° (SD: 10.5), while tributaries underlain by sedimentary bedrock have an average gradient of 13.3° (SD: 11.9).

4.2. Precipitation and Streamflow

The cumulative rainfall was 505 and 557 mm in the 2021 and 2022 water years, respectively. Based on a 36 year record from a nearby weather station (Haskins Ranch, Santa Clara Valley Water), 2021 precipitation was <tenth

Table 1
Catchment Metrics Averaged Across North Dark Canyon and South Dark Canyon Catchments and Mélange and Sedimentary Areas (See Figure 1 for Site Map)

Topographic metrics	North dark canyon	South dark canyon	Mélange (NDC only)	Sedimentary (NDC and SDC)
Total catchment area (km^2)	0.77	0.91	-	-
Mean elevation (m amsl)	722.17	745	705.26	739.48
Mean topographic slope (°)	23.6	24.6	21.3	25.3
Mean channel slope (°)	13.4	13.6	16.5	13.3
Mean profile curvature (1/m)	-2.77×10^{-5}	-4.62×10^{-5}	-3.20×10^{-5}	-3.13×10^{-5}
Drainage density (km/km^2)	7.5	5.8	11.1	6.2

percentile, and 2022 precipitation was <25th percentile for the region. A majority of streamflow, especially at NDC, was associated with atmospheric river events that had precipitation totals >100 mm. For example, the largest precipitation event in the 2021 water year totaled 140 mm of rainfall. Over the 4.4 day period between the start of that event and the beginning of the next precipitation event (26th–29th January, 2021), NDC exported 84% of the annual streamflow, and SDC exported 14% of the annual streamflow.

Table 2
Summary Table of Mean Concentrations, Concentration-Discharge Slopes, and CV_c/CV_Q Values of Sampled Waters

NDC surface water								
Analyte	n	Mean C (mg/L)	b (All years)	b (2021)	b (2022)	CV_c/CV_Q (all years)	CV_c/CV_Q (2021)	CV_c/CV_Q (2022)
Ca^{2+}	122	26.89	−0.03	0.05	−0.13	0.11	0.12	0.17
Na^{+}	122	14.33	−0.11	−0.08	−0.18	0.14	0.14	0.23
Mg^{2+}	122	13.05	−0.11	−0.08	−0.19	0.14	0.12	0.22
$SO4^{2-}$	126	28.64	−0.12	−0.08	−0.21	0.18	0.22	0.24
K^{+}	122	2.16	0.06	0.08	0.03	0.13	0.15	0.17
Cl^{-}	126	12.69	−0.10	−0.06	−0.14	0.18	0.24	0.22
DOC	103	9.57	0.17	0.20	0.33	0.31	0.29	0.38
SDC surface water								
Analyte	n	Mean C (mg/L)	b (All years)	b (2021)	b (2022)	CVc/CVQ (all years)	CVc/CVQ (2021)	CVc/CVQ (2022)
Ca^{2+}	96	27.29	−0.08	−0.03	−0.09	0.28	0.24	0.21
Na^{+}	96	20.82	−0.09	−0.12	−0.10	0.20	0.16	0.27
Mg^{2+}	96	12.74	−0.11	−0.12	−0.17	0.22	0.19	0.27
$SO4^{2-}$	95	27.64	−0.13	−0.16	−0.16	0.40	0.31	0.48
K^{+}	96	1.62	<0.01	−0.02	0.01	0.33	0.30	0.39
Cl^{-}	95	17.55	−0.17	−0.13	−0.09	0.38	0.31	0.28
DOC	87	6.82	0.05	0.11	0.05	0.84	0.43	0.86

	NDC seeps		SDC seeps		Precip.	
Analyte	n	Mean C (mg/L)	n	Mean C (mg/L)	n	Mean C (mg/L)
Ca^{2+}	13	43.10	11	38.15	7	3.60
Na^{+}	13	23.10	11	27.18	7	0.90
Mg^{2+}	13	20.54	11	14.65	7	0.31
$SO4^{2-}$	13	37.39	11	15.69	8	0.52
K^{+}	13	2.89	11	2.24	7	0.84
Cl^{-}	13	16.82	11	21.62	8	1.11
DOC	9	1.46	4	1.45	3	5.23

10.1029/2024WR037086

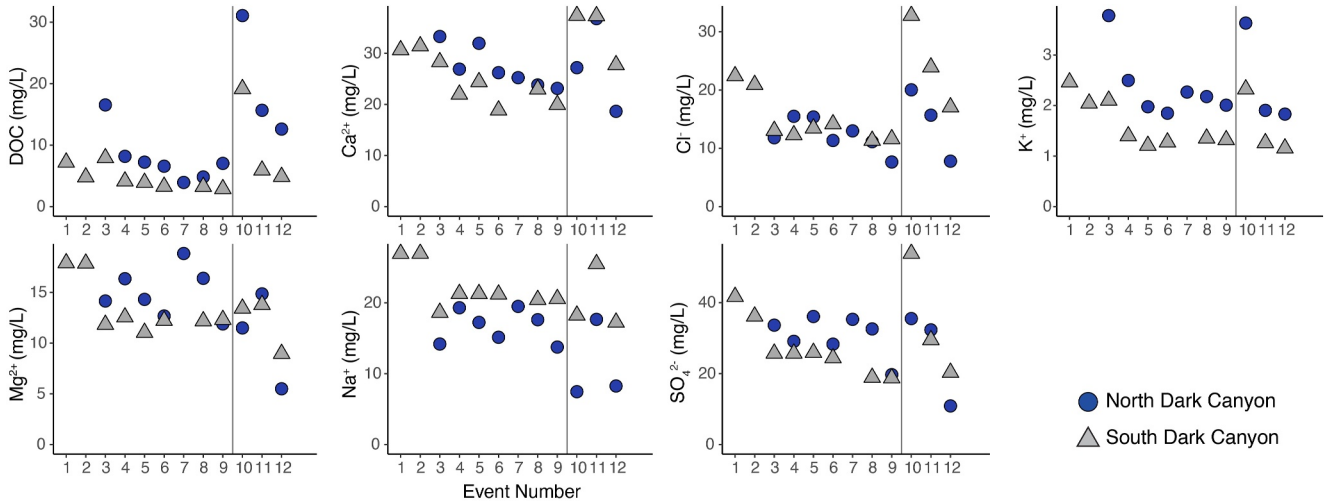

Figure 3. Event mean concentration (MC) values for each streamflow event in 2021 and 2022. The vertical black line denotes the start of a new water year; events 1–9 occurred in the 2021 water year, and 10–12 occurred in the 2022 water year. North Dark Canyon values are represented by blue circles and South Dark Canyon values by gray triangles.

The precipitation water chemistry of sampled rain events had low concentrations of Mg^{2+} and SO_4^{2-} (non-weighted average < 0.6 mg/L). K^+ concentrations averaged 0.84 mg/L (SD): 1.5). Non-weighted average concentrations of Cl^- were 1.1 mg/L (SD:1.1) and 0.9 mg/L (SD: 1.0) for Na^+. Ca^{2+} concentrations averaged 3.6 mg/L (SD: 2.0). The MC of DOC in the subset of precipitation samples with sufficient volume for all analyses was 5.2 mg/L (SD: 3.2).

Streamflow at the catchment outlets was highly seasonal. However, streamflow out of NDC displayed much flashier behavior than the adjacent SDC stream (Figure 2). At the NDC outlet, flow only occurred for 29% of the study period, while SDC maintained flow for 68% of the study period (2021 and 2022 water years). Mean peak streamflow values (<1% exceedance) were 7.8 times higher at NDC than SDC. North Dark Canyon had 10 streamflow events during the study period (denoted as events 3–12 in Figure 2), and SDC had 14 streamflow events. In the 2021 water year, NDC exported 38 mm, and SDC exported 23 mm of streamflow. In the 2022 water year, NDC exported 24 mm, and SDC exported 21 mm of streamflow. The streamflow recession rates were faster in NDC than SDC, with a recession slope of 0.94 at NDC and 0.77 at SDC.

4.3. In-Channel Seeps and Perennial Stream Reaches

In the dry season (June-September), the entire NDC stream network dried down except at six small (<0.5 m) stagnant pools at groundwater seeps. In contrast, SDC sustained flow across multiple short (3–10 m) perennial reaches in addition to two stagnant pools at seeps (Figure 1). We assume water from summer seeps represents groundwater discharge. Overall, NDC seep samples had 2.4 times higher mean concentrations of SO_4^{2-} and 1.4 times higher concentrations of Mg^{2+} when compared to SDC seep samples (Table 2). At NDC, the seep samples had higher concentrations of Na^+, Mg^{2+}, and Ca^{2+} compared to all surface water samples collected at the outlet of NDC (Table 2). At SDC, seeps were more saturated with Na^+ and Ca^{2+} and less saturated with SO_4^{2-} when compared to all surface water samples at the SDC outlet.

4.4. Surface Water DOC Concentrations and C-Q Patterns

Concentrations of DOC at NDC were variable, ranging from 2.53 to 35.4 mg/L. Concentrations of DOC at SDC ranged from 1.85 to 26.7 mg/L. Event mean concentrations (MCs) at NDC ranged from 3.94 mg/L to 31.1 mg/L, and MCs at SDC ranged from 3.25 mg/L to 19.2 mg/L. In both water years, NDC displayed strong seasonality, with the highest DOC concentrations occurring in the first flow activation event during the fall/winter wet-up period. In NDC, DOC MCs peaked at 16.5 mg/L and 31.2 mg/L during the first flow events of 2021 and 2022, respectively. The MCs during each subsequent event generally decreased (Figure 3). MCs of DOC at SDC generally were lower and less variable than NDC. At SDC in the 2021 water year, MCs of DOC were highest

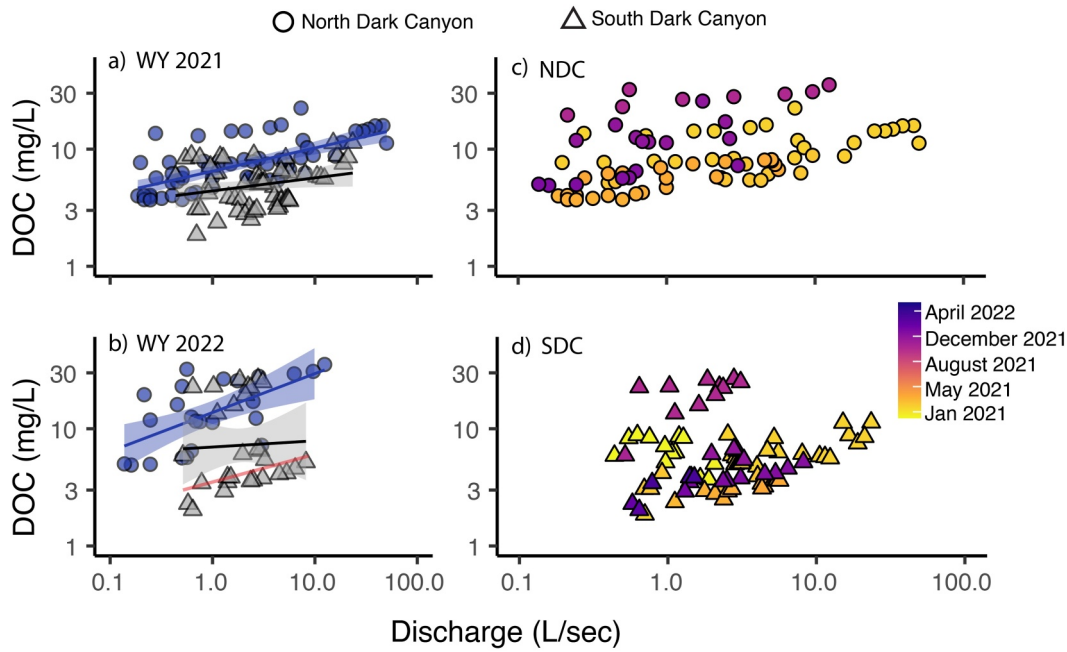

Figure 4. Concentrations - discharge plots of dissolved organic carbon at North Dark Canyon (NDC) and South Dark Canyon (SDC) outlets. (a, b) concentration-discharge (C-Q) slopes separated by water year and colored by sample location, with dark blue circles indicating NDC and gray triangles indicating SDC. The C-Q slopes (dark blue line) at NDC in (a) 2021, and (b) 2022 are 0.20 and 0.33 respectively, and SDC slopes (black line) in 2021 (a) to 2022 (b) are 0.11 and 0.05 respectively. The light red line shows the C-Q relationship if the October 2021 event (Event 10) is removed, changing the slope from 0.05 to 0.20. (c, d) Panel c shows all NDC samples, and panel d shows all SDC samples with both panels colored by date. These are the same samples from a/b, now subset by sample location instead of water year.

during the third event (7.91 mg/L). This event was also the highest discharge event observed in SDC (peak flow: 24 L/s). At SDC in the 2022 water year, DOC peaked during the first flow event of the year (19.2 mg/L) and decreased in the subsequent sampled events. However, due to instrument failure, we do not have samples from the largest discharge event of the 2022 water year, so DOC response is uncertain during this event.

North Dark Canyon and SDC had distinct DOC C-Q relationships at inter-annual and annual time scales (Figure 4). The C-Q slope of DOC at NDC, determined using samples collected in both water years, was 0.17, and at SDC was 0.05. In the 2021 water year, the C-Q slope at NDC was borderline chemodynamic ($|b| > 0.20$) and positive ($b = 0.20$; p-value <0.001), while SDC was more chemostatic ($b = 0.11$, p-value = 0.055). In the 2022 water year, the C-Q slope at NDC was more strongly chemodynamic and positive ($b = 0.33$; p-value <0.001). While SDC was strongly chemostatic ($b = 0.05$; p-value = 0.89).

During the October 2021 event, despite high rain intensities and considerable DOC mobilization, peak discharge at SDC only reached 3.1 L/s. We also observed considerable DOC mobilization at NDC, however discharge reached 28 L/s (Figure 4). While SDC displayed positive C-Q behavior later in the water year, the overall C-Q slope was constrained by this October event, driving a negative slope and chemostatic behavior. Excluding this event, SDC's 2022 C-Q slope changes from 0.05 to 0.20 and increases the C-Q slope of all SDC samples from 0.05 to 0.14. At the event scale, C-Q slopes at SDC tended to be steeper and more variable than across the entire water year, ranging from −0.21 to 0.6. While NDC event C-Q slopes are more consistent and often slightly lower than the annual scale C-Q slopes, ranging from −0.08 to 0.17.

4.5. Surface Water Major Ion Concentration and C-Q Patterns

Over the entire study period, surface water concentrations of major ions were similar at both catchments (Table 2). At NDC, the dominant mean ion concentrations were $SO_4^{2-} > Ca^{2+} > Na^+ > Mg^{2+} > Cl^- > K^+$. At SDC, the dominant ions were $SO_4^{2-} > Ca^{2+} > Na^+ > Cl^- > Mg^{2+} > K^+$. In all years, the mean concentrations of Cl^- and Na^+ were statistically higher at SDC than at NDC. No other ion concentrations were statistically different

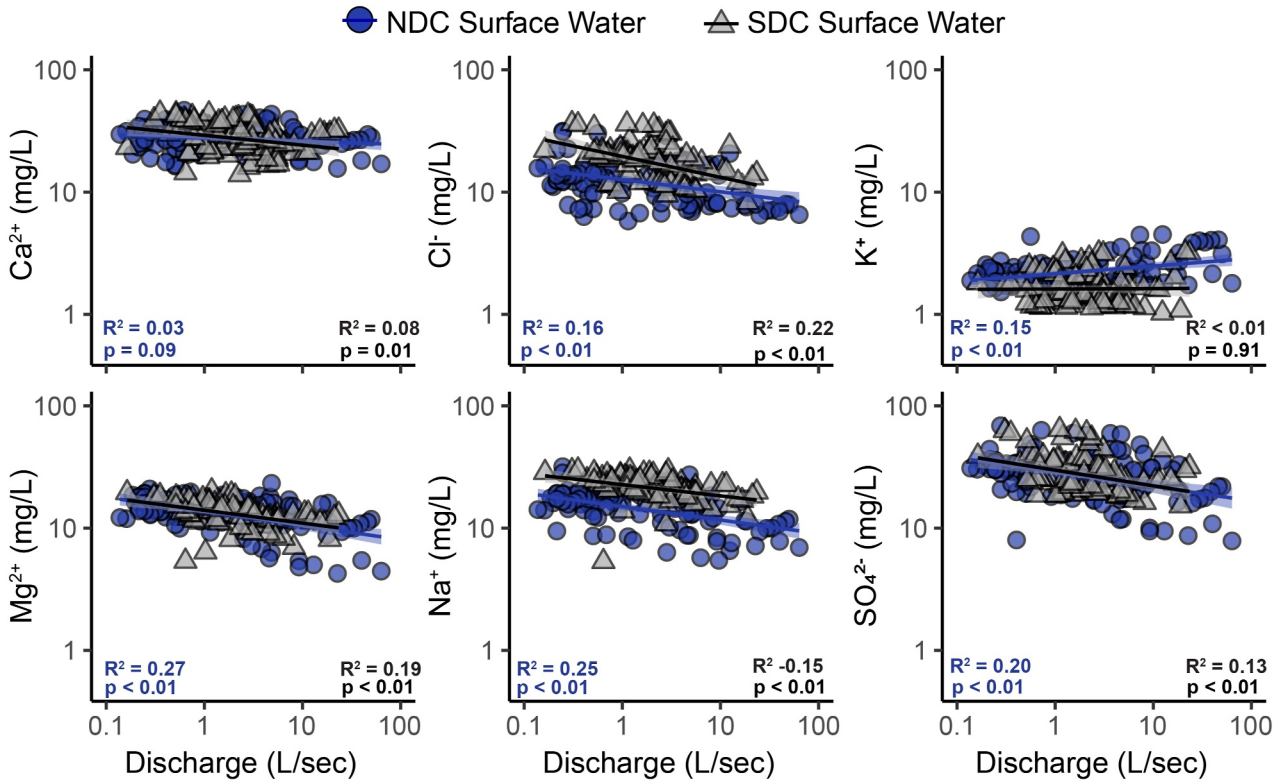

Figure 5. Concentrations - discharge (C-Q) plots with all major ions samples collected during the study period at North Dark Canyon (NDC) and South Dark Canyon (SDC) outlets. NDC samples are indicated by blue circles and SDC samples are indicated by gray triangles. Slopes of C-Q relationships are shown by the linear regression lines; blue lines fit NDC samples, and black lines fit SDC samples. All C-Q slopes are negative except K^+, which has a slight positive slope (0.06 and <0.01 at NDC and SDC, respectively). R^2 and p-values text colors follow the same patterns described above.

between catchments for the 2021 and 2022 water years (Table 2). The variability in event MCs of Ca^{2+}, Cl^-, and K^- at both catchments tended to be greatest during the first 1–2 streamflow events of the season (Figure 3). For Na^+, $SO4^{2-}$, and Mg, variability in event MCs was not consistent year-to-year.

The C-Q slopes of each ion species were almost always chemostatic, regardless of whether the samples were binned by the event scale, annually, or all samples (Table 2; Figure 5; Figure 6). When major ion C-Q slopes were calculated using samples from the entire study period, they ranged from −0.17 to <0.01 at SDC and from −0.12 to 0.06 at NDC (Figure 5). The steepest slope at SDC was observed in Cl^- (−0.17), and the steepest slope at NDC was observed in SO_4^{2-} (−0.12). The C-Q relationship of ions in both catchments (except Ca^{2+} at NDC and K^+ at SDC) had statistical significance (p-value <0.05; Tables S1 and S2 in Supporting Information S1). When C-Q slopes were binned by water year, relationships were mostly similar; nearly all annual C-Q slopes remained slightly negative and chemostatic. However, slopes did tend to be slightly more negative in 2022, especially at NDC. Notably, SO_4^{2-} surpassed the chemostatic threshold with weak dilution behavior ($b = -0.21$).

At the event scale, C-Q relationships of major ions still tended to be chemostatic (Figure 6) with short periods of chemodynamic behavior for some solutes. Additionally, for large streamflow events (events that exported 25% or more of the annual streamflow), the C-Q slopes were almost always negative at both catchments. Notable exceptions to chemostatic behavior were observed in SO_4^{-2} during the January 2021 event (labeled Event 3) and December 2021 event (labeled Event 12) at NDC, which displayed weak dilution behavior slopes of −0.24 and −0.22, respectively. The December 2021 event (labeled event 12) at SDC also showed weak dilution behavior in SO_4^{-2} (b: −0.21) and Mg^{2+} (−0.23). Additionally, the October 2021 event (Event 10), which only represents 1.2% of the annual streamflow, showed strong flushing behavior at SDC with C-Q slopes ranging from 0.27 to 0.52. Occasionally, other solutes in small events also surpassed the chemostatic threshold at SDC, such as Ca^{2+} during the December 2020 event at SDC (labeled event 2), which had a C-Q slope of −0.29 and K^+ during a December 2021 event (labeled event 11) which had a C-Q slope of 0.41. At NDC, event scale C-Q behavior of

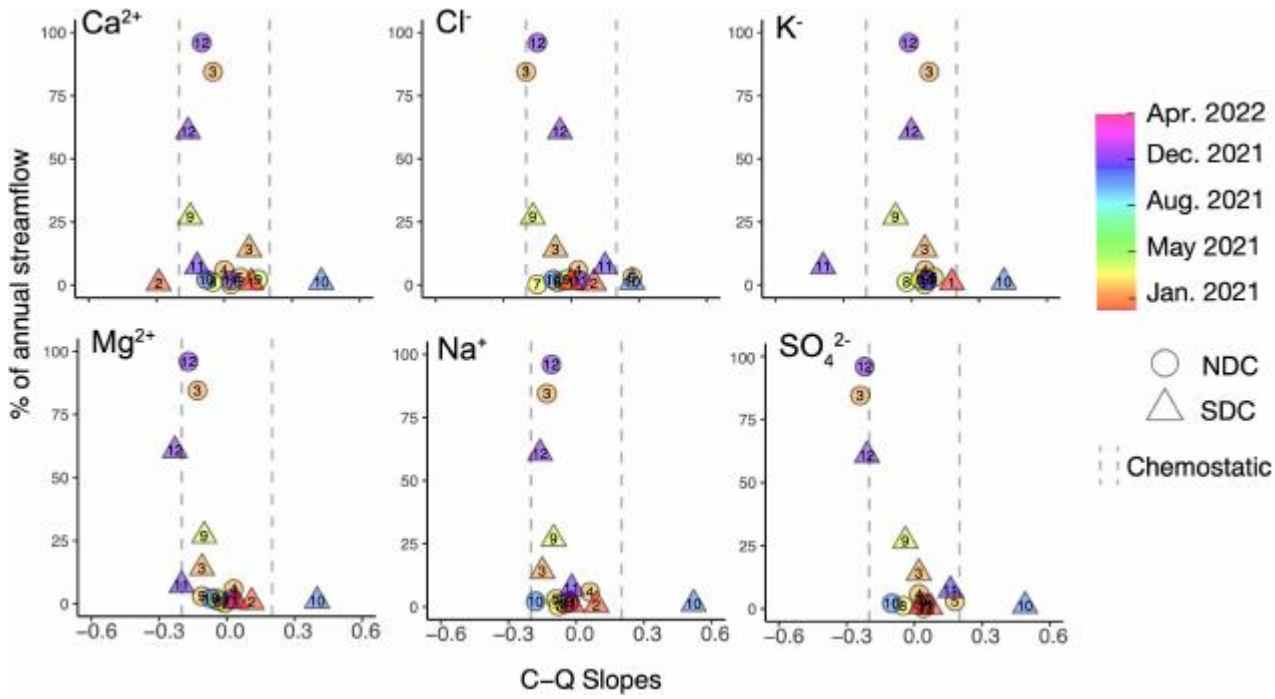

Figure 6. Event scale concentration-discharge (C-Q) slopes of major ions at North Dark Canyon (circles) and South Dark Canyon (triangles). The chemostatic range is indicated by vertical dashed lines where most events fall, C-Q slopes >0.2 have flushing behavior and C-Q slopes < −0.2 have dilution behavior. Events are colored by date and labeled with the event number.

Ca^{2+}, Mg^{2+}, Na^{+}, and K^{+} at were always chemostatic. The event C-Q slopes at SDC were more variable than NDC, with some solutes (Ca^{2+}, Mg^{2+}, K^{+}, and SO_4^{2-}) showing both flushing behavior and dilution behavior at different points in time. However, a majority of events at both catchments still displayed chemostatic behavior.

5. Discussion

5.1. Short and Shallow Versus Long and Deep: Lithologic Controls on Hydrologic Flow Paths and Streamflow Behavior

Our observations of streamflow behavior at NDC and SDC fit within the previously developed frameworks of mélange and sedimentary bedrock's critical zone structure and hydrologic behavior in other nearby California field sites (Dralle et al., 2023; Hahm et al., 2019) and broader frameworks describing the role of upland hillslope contributions to streamflow (Li & Ameli, 2023). Our direct observations of subsurface characteristics and groundwater at BORR are mostly limited to one 0.04 km^2 catchment (termed "Arbor Creek Experimental Catchment") that drains to NDC, underlain by sedimentary bedrock (Callahan et al., 2024; Donaldson et al., 2023, Figure 1). Donaldson et al. (2023) characterized the soil, saprolite, and shallow groundwater across a study transect in Arbor Creek. They observed perched groundwater at the soil to saprolite transition (3–4 m below the surface) periodically during the 2021 rainy season (January to May). Additionally, Callahan et al. (2024) extended critical zone observations beyond the saprolite in Arbor Creek and observed extensive fracturing and depths to fresh sedimentary bedrock between 24.7 and 36.6 m below the ground surface at ridgetops, depending on borehole location. At the transition from oxidized to fresh bedrock, they also observed the perennial groundwater during the 2023 water year that rose above the ground surface in Arbor Creek's stream channel during periods of high rainfall. It is unclear how hydrologically connected this perennial groundwater system is to surface water in the study catchments during periods of low rainfall. Regardless, these observations suggest that the critical zone properties of sedimentary hillslopes allow for high water storage and various subsurface hydrologic flow paths, including transient shallow groundwater and deeper groundwater contributions. In SDC, higher water storage capacity likely contributes to the prolonged presence of baseflow (Figure 2) and short reaches of perennial surface water in SDC's mainstem (Figure 1).

Critical zone characterization in mélange bedrock at BORR was done through geologic mapping and geophysical observation of seismic velocities through two mélange-sedimentary transects (Figure 1; Text S2 in Supporting Information S1; Figures S3 and S4 in Supporting Information S1). At the surface, boulder-sized outcrops of chert and blueschist are scattered on the landscape, surrounded otherwise by soil-mantled hillslopes, with occasional greywacke and shale outcrops along stream channels. Preliminary geophysical work was run along hillslope transects with no visible chert or blueschist boulders. Generally, the mélange regions of the seismic lines showed slightly shallower depths to bedrock (19.75–25.25–2500 m/s velocities) compared to the sedimentary regions (27.75–31.75–2500 m/s velocities). However, these geophysical observations are limited in spatial extent and do not capture the full range of rock types observed across NDC's mélange hillslopes. Compared to our observations, Hahm et al. (2019) observed the depth to fresh bedrock as shallow as 3 m at ridge tops. However, NDC's hillslopes are much more heterogeneous and have a larger fraction of sandstone and shale than is observed in their study. Despite potential discrepancies in bedrock depth across mélange in these studies, our observed streamflow behavior is similar to other studies along the Eel River, which indicates shallow flow paths and limited vertical recharge, evidenced by extremely flashy streamflow and limited surface water in the dry season. Additionally, we observed higher variability in runoff year-to-year at NDC (2021: 38 mm, 2022: 24 mm), while SDC runoff was more consistent (2021: 23 mm, 2022: 21 mm), which also may suggest a lower storage capacity in NDC hillslopes that is responsive to year-to-year variability in precipitation. Li and Ameli (2023) also present a generalizable framework for understanding variations in low-flow recession rates and drought vulnerability. They show that rapid recession rates, such as the observations at NDC, are driven by limited water subsidies from upland hillslopes. In contrast, catchments with slower recession rates, such as SDC, suggest larger contributions from deep, slow-moving, upland hillslopes. While critical zone differences between mélange and sedimentary hillslopes may be more subtle or inconclusive at BORR than other California landscapes, they still give rise to distinct differences in streamflow, recession, and drought vulnerability.

In addition to the subsurface critical zone's controls on streamflow behavior, high drainage density on mélange hillslopes reflects NDC's tendency toward flashy streamflow and suggests short, shallower flow paths (Table 1). Stream channels represent the fastest hydrologic flow path through a landscape, and higher channel densities reduce the residence time of water in the subsurface (Patton & Baker, 1976). Additionally, landscapes evolve such that higher drainage densities occur in conjunction with shallower hydrologic flow paths (Jefferson et al., 2010; Litwin et al., 2024; Yoshida & Troch, 2016). The drainage density at our field site is highest in the portion of the catchment underlain by mélange (Table 1). Topography, climate, vegetation, and lithology have been shown to influence channel density across a range of landscape types and climate zones (Carlton, 1963; Gregory & Walling, 1968; Luo et al., 2016; Sangireddy et al., 2016). Given the similarities across our two study catchments, we suggest that drainage density is likely lithologically controlled. Together, the subsurface critical zone and channelization point toward shallow and short hydrologic flow paths in NDC's mélange hillslopes, contrasting with deeper, longer, and more variable hydrologic flow paths at SDC.

5.2. DOC Observations Suggest Shallower Hydrologic Flow Paths in NDC's Mélange Hillslopes

Overall, the DOC export behavior at both catchment outlets matches observations across a range of other studies, where DOC concentrations increase with increasing discharge (Moatar et al., 2017; Raymond & Saiers, 2010; Zarnetske et al., 2018). Additionally, high concentrations of DOC are commonly observed following drought periods and during high-intensity rainfall events (Bernal et al., 2002, 2013; Vázquez et al., 2007), which also aligns with our observations of the re-wetting behavior in these intermittent stream channels. Specifically, we observed the highest mean concentrations of DOC in the first major flow events of the water year, following extended periods with no rain, and the highest DOC event MCs of the study period during the October 2021 event, with rainfall intensities reaching up to 21.8 mm/hr. While the DOC export patterns at both catchments were broadly similar to other studies, concentrations of DOC were consistently higher at NDC.

The DOCexport behavior at the NDC outlet further supports our hypothesis that shallow flow paths drive water and biogenic material export behavior in this catchment. Dissolved organic carbon has been shown to be largely derived from shallow hydrologic flow paths through the organic-rich soil zones, where plant biomass, roots, and microbes are abundant (Bowering et al., 2020; Jobbágy & Jackson, 2000; Ploum et al., 2020; Wu et al., 2024). On average, the event concentrations were 1.8 times higher in NDC than in SDC. The DOC concentrations at NDC were highest during the first event of the water year and generally decreased with each subsequent event. During this first event, substantial DOC is likely flushed from the shallow subsurface and the previously dry stream

channels (Inamdar et al., 2012; Raymond & Saiers, 2010; Strohmeier et al., 2012). In subsequent events, shallow, near-, and within-stream DOC sources likely become depleted, with a majority of the shallow DOC pool already mobilized. At SDC, while high DOC export was also observed in the first flow event, event concentration event concentrations of DOC did not decrease as strongly across the water year. At SDC, peak DOC concentrations appeared to have a stronger connection with precipitation event size, and DOC sources were not as readily depleted. Variability in the distribution and abundance of DOC in catchments can also contribute to DOC export patterns (Herndon et al., 2015), particularly riparian zones with higher biomass tend to build higher soil organic carbon and can contribute to higher DOC in streams (Aitkenhead et al., 1999; Dosskey & Bertsch, 1994; Fiebig et al., 1990). However, both NDC and SDC stream channels are surrounded by steep hillslopes, and NDC has limited to no flat-lying riparian or wetland zones along the stream channel, suggesting hydrologic flow paths through shallow soil is the dominant DOC source in NDC. While SDC does have some small and moderately flat riparian zones, indicated in Figure 1 by "Valley fill (Qf)," which may contribute to DOC export at the outlet, the DOC concentrations at SDC are still limited compared to NDC. Thus, variability in the distribution and abundance of DOC does not appear to be a dominant driver of DOC export patterns. However, the characterization of water from various subsurface stores and soil properties could further illuminate the carbon pools and biogeochemical processes influencing DOC export in each catchment.

5.3. Mechanisms for Chemostatic Behavior at NDC and SDC Catchments

Generally, we expect higher solute concentrations of weathering-derived solutes to be associated with longer residence times in a catchment, where long residence times allow sufficient time to reach thermodynamic limits or overcome buffering processes (Ameli et al., 2016; Maher, 2010, 2011; Stewart et al., 2022). As a result, we expected SDC would have higher mean concentrations of most major ions due to its apparent stronger connection to deeper, longer hydrologic flow paths. However, higher mean concentrations at SDC were only observed in Na^+ and Cl^- (Table 2), while all other major ions were similar between catchments. Additionally, we expected major ions to be more chemostatic in SDC, assuming ion-saturated groundwater would make up a larger proportion of streamflow in SDC, reducing the effect of dilution (Stewart et al., 2022). This was also not observed, with C-Q slopes generally similar across both catchments and largely chemostatic across most analytes regardless of the C-Q timescales (Ameli et al., 2016, Table 2; Figure 5; Figure 6). We also note that the determination of chemostasis based on CV_c/CV_Q values (threshold 0.5) results in similar conclusions of broadly chemostatic behavior (Table 2; Tables S1 and S2 in Supporting Information S1).

We hypothesize that the observed inter-annual and annual chemostatic behavior across our two study catchments may occur because solutes are readily mobilized in the critical zone, regardless of the perceived depth of dominant hydrologic flow paths. Similarities in the mean concentrations of most major ions across our study catchments (Table 2) may be driven by broadly similar geochemistry (Hahm et al., 2019) and the dominance of silicate weathering in both bedrock lithologies. Godsey et al. (2009) suggested that chemostatic behavior could be explained by invoking the concept that permeability, porosity, and pore aperture exponentially increase toward the surface. Thus, as a catchment wets up and water tables rise, higher reactive surface areas and higher reaction rates buffer stream chemistry, driving chemostatic behavior. This is supported and expanded by several studies that have shown that incoming rainfall can rapidly acquire major ions in the vadose zone from rapid cation exchange, dissolution of secondary minerals and clays, and release of trapped ions. For example, Cartwright et al. (2020) saw chemostatic behavior despite distinct reductions in mean transit times and suggested chemostasis occurred due to similar concentrations of major ions in soil water and baseflow. This is similar to other studies that showed that up to 50%–74% of the solutes in stream water are generated in the vadose zone by rapid cation exchange and dissolution of secondary minerals driven by high pCO_2 in rainfall (Anderson et al., 1997; Kim et al., 2017). In both NDC and SDC catchments, water may rapidly acquire major ions in the subsurface. Transitions between layers in the subsurface (e.g., soil horizons, saprolite, weathered bedrock, fresh bedrock) and the associated changes in permeability or hydraulic conductivity create short-term saturated zones that deliver water and dissolved ions to the stream (Ehrhardt et al., 2022; Heller & Kleber, 2016; Zimmer & McGlynn, 2018). Additionally, while the depth of saturated zones in the subsurface may differ in NDC and SDC, streamflow in both catchments is likely dominated by pre-event water (Buttle, 1994; Clow & Mast, 2010; Sklash & Farvolden, 1979). Even in other landscapes with mélange bedrock, where the dominant stream runoff generation mechanism has been shown to be overland flow, peak stormflow was still dominated by pre-event water (Lapides et al., 2022). Together, the dominance of pre-event water and high cation exchange processes suggest that even

fast, shallow hydrologic flow paths may have sufficient conditions to acquire ions and thus drive the chemostatic behavior we observed in NDC. That said, we did observe dilution behavior during periods of very high saturation or overland flow (Figure 6), suggesting there are short periods when water influx outpaces the subsurface capacity or chemical reaction rates, and dilute water contributes to the stream as overland or shallow subsurface flow.

The C-Q behavior of major ions is complex because each ion is uniquely influenced by atmospheric deposition, cation exchange, plant uptake, microbial activity, leaching, and mineral weathering to various degrees (Ameli et al., 2016; Crowther et al., 2019; Herndon et al., 2015; Lindberg et al., 1986). Here, we discuss specific processes that may influence ions associated with salt and clay dissolution. A reactive transport model developed at the Susquehanna Shale Hills CZO (Li et al., 2017) showed chemostasis of Cl^- occurred due to the trapping of Cl^- in soil water during periods of elevated evapotranspiration and decreasing streamflow (e.g., spring and summer), that was subsequently mobilized as the catchment wet up in fall. Potential differences in the timing and sources of plant water use could create differences in the extent and patterns of salt exclusion between NDC and SDC and help explain elevated Cl^- and Na^+ in SDC stream water, which was characterized by peaks during the fall wet-up period. The reactive transport model also showed that Mg^{2+} chemostasis occurred due to higher clay dissolution during periods of high volumetric water storage, increasing the mineral reactive surface area. In addition to Mg^{2+}, Ca^{2+}, and Na^+ are common cations in clay minerals. Clay dissolution may also help explain chemostatic behavior in NDC and SDC as well. Together, broadly similar bedrock geochemistry, streamflow dominated by pre-event water, and rapid chemical reactions in the critical zone likely drive similar annual mean concentrations of major ions and limited changes in surface water chemistry over a broad range of flow conditions in both catchments.

Further analyzing event-scale C-Q patterns may provide some additional insight into the hydrologic controls on solute export (Speir et al., 2024). While event C-Q patterns of major ions still tended to be chemostatic at both catchments, C-Q slopes did tend to be more variable and steeper at event scales than annual and inter-annual scales, especially at SDC (Figure 6). Higher variability in event-scale C-Q patterns compared to annual and inter-annual patterns has been attributed to meteorological and anthropogenic influences like dry and wet deposition (Knapp et al., 2020) and variability in hydrologic connectivity (Rose et al., 2018). At SDC, we observed a trend in event scale C-Q behavior, where the C-Q slopes tend to be positive early in the water year and trend toward steeper negative C-Q slopes as the water year progresses, especially for Cl^-, Mg^{2+}, Na^+, SO_4^{2-} (Figure 6). This trend may indicate higher groundwater contributions to streamflow and/or flushing of accumulated materials in the streambed early in the water year with progressive wet up and contribution from shallower hydrologic flow paths later in the water year, contributing toward dilution (Rose et al., 2018). This contrast of early season positive C-Q slopes and late-season negative C-Q slopes also likely contributes to the annual and inter-annual chemostatic behavior at SDC. Variations in event scale C-Q slopes at NDC also likely reflect antecedent wetness conditions and hydrologic connectivity. However, NDC's event scale C-Q slopes tended to be less steep and less variable, which may reflect more consistency in NDC's hydrologic flow paths through time. While more work characterizing the subsurface water chemistry in both catchments is needed, analyzing solute export between the two catchments at event scales shows variability in solute export between catchments that is not apparent at longer time scales. Additionally, these observations suggest equifinality, with potentially different combinations of mechanisms resulting in the same observation of chemostatic behavior across the study catchments. As others have also noted, we conclude that more work capturing water from various subsurface depths and age distributions is needed to tease apart drivers (Ameli et al., 2021; Knapp & Musolff, 2024).

5.4. The Role of Wildfire Disturbance and Extreme Events on Stream Water Chemistry and Discharge Behavior

To aid in the transferability of our findings to other studies, it is important to couch our results and interpretations in the context of the unique site history, past disturbance, and the precipitation regime of this site. In particular, this field site experienced a low-to-moderate intensity wildfire in August 2020. Our study took place in the 2021 and 2022 water years; thus, the observed DOC concentrations and export dynamics may be influenced by wildfire disturbance. It is important to note that wildfire intensity has been shown to strongly influence subsequent in-stream DOC export. For example, high-intensity wildfires generally cause a decrease in DOC concentrations (Wei et al., 2021), while moderate-severity fires can increase DOC concentrations in streams following wildfires (Uzun et al., 2020). However, it is challenging to determine the impact of this low-severity fire in these study catchments without sufficient pre-fire data. Regardless, we believe the DOC export behavior still gives insight

into the dominant hydrologic flow paths through the landscape, considering the fire burned 100% of both catchments at similar intensities and with similar fuel types.

The precipitation regime at this study site is characterized by winter rain, where the majority of rain occurs during large but relatively infrequent atmospheric river events. As discussed previously, the DOC C-Q slope at SDC was highly influenced by one streamflow event. The October 2021 streamflow event was the first major precipitation event of the 2022 water year, delivering >140 mm in 38 hr (26% of total annual precipitation). This event showed positive but chemostatic C-Q behavior, with an event-scale C-Q slope of 0.16 (p-value: 0.32). Additionally, the 10 highest DOC samples collected over the entire 2-year study period at SDC were collected during this event. However, discharge only reached 3 L/s (max Q observed over the entire study period was 52 L/s). While less distinct, a similar event occurred at the start of the 2021 water year, where discharge values only reached 1.8 L/s but had the second-highest event MC of DOC in the 2021 water year. As a result, the C-Q relationship at both the annual and interannual timescales were constrained by these two-fall wet-up events, causing the C-Q relationship at SDC to appear more chemostatic. We showed that removing events such as these can cause the C-Q slope to change dramatically for DOC, where the chemostatic C-Q slope (0.05) during the 2022 water year at SDC became 0.20 with the removal of these data points (Figure 4). High DOC export during these events was likely due to the mobilization of near- or within-stream DOC after several dry months. At SDC, a considerable portion of this first incoming rain event likely contributed to the recharge of intermediate or deeper groundwater. This is evident from the limited streamflow during the precipitation event and the continuation of baseflow for several weeks after. We suggest that the C-Q relationships of DOC and other biologic solutes require careful consideration of event-scale dynamics and timing of precipitation to be meaningfully interpreted (Creed et al., 2015). These dynamics also highlight the significance of sample timing, as an early season rainfall event can be easily missed in sampling efforts and have longstanding impacts on long-term C-Q relationships and interpretations.

5.5. Limitations and Future Directions

Given variability in the definition of "chemostatic" versus "chemodynamic" behavior across literature, we briefly discuss how different methodological decisions would influence our interpretations. Choosing a C-Q slope cutoff value of ±0.1 instead of the ±0.2 we used in our analysis (Stewart et al., 2022) would result in a larger fraction of major ions displaying "chemodynamic" behavior in this study, especially at SDC. However, using a CVc/CVQ value of 0.5 in this study would suggest a majority of major ions at both catchments have "chemostatic" behavior consistent with our results. We do note that SDC consistently has higher CVc/CVQ values (though generally still below 0.5) driven by lower magnitude, muted streamflow responses. Therefore, the use of a different chemodynamic threshold value may have suggested that NDC is more consistently chemostatic, further highlighting the influence of rapid chemical reactions in the shallow critical zone on surface water chemistry. Regardless of the thresholds used to define chemostatic behavior, major ion concentrations are still considerably less variable than discharge and often less variable than biogenic solutes at both catchments, thus consideration of major ion buffering is still necessary. We also showed that individual streamflow events can have outsized impacts on C-Q relationships. Therefore, we recommend consideration of event-scale patterns to help tease apart drivers and to ensure the C-Q relationship is representative of the time scale of interest.

The analyses and critical zone-informed framework used here could be expanded in future studies in several ways. While the similarities in our two study catchments (topography, climate, vegetation, etc.) aid in controlling for the role of lithology, using datasets that capture longer-term solute export dynamics and bringing together data sets from other regions with high lithologic and hydrologic variability would contribute to a more generalizable framework for describing the role of subsurface structure on solute export. Further, as discussed in Section 5.3, samples collected at catchment outlets integrate chemical signals from various hydrologic stores and ages. Thus, it is extremely challenging, especially at event scales, to differentiate which of the various transport and biogeochemical mechanisms discussed above are driving C-Q patterns at the catchment outlet at specific times. As described in Knapp and Musolff (2024), an important next step for C-Q research is to systematically and empirically test our hypotheses for emergent C-Q relationships. To do this, future studies should consider pairing stream water chemistry with soil or groundwater chemistry, water observations in these stores, as well as transit time distribution modeling or process-based modeling. Finally, as this study spanned only two water years per catchment, there is utility in long-term studies that cover a wider range of hydroclimatic variability. While overcoming the high heterogeneity of subsurface properties poses ongoing challenges, these future directions would strengthen the interpretability of C-Q patterns at catchment outlets and improve the predictions of C-Q patterns at event scales.

6. Implications and Conclusions

Differences in surface water persistence and streamflow response are driven by distinct subsurface hydrologic flow paths. Our results contribute to other research showing that catchments underlain by mélange bedrock have much more ephemeral streamflow behavior than adjacent headwater catchments with different lithology despite similar topography, climate, and vegetation. Despite these hydrologic differences, mean concentrations of in-stream major ions were similar, and C-Q relationships were chemostatic at both catchments, likely driven by rapid cation exchange processes and/or a high fraction of pre-event water in streamflow. We show that annual DOC export patterns in these non-perennial headwater catchments can be highly influenced by individual storm events due to sporadic and limited precipitation events and seasonal controls on DOC supply.

Our results connecting lithology to catchment export dynamics have implications for water resource management in California and other arid and semi-arid rain-dominated regions. The mélange bedrock played an outsized role in a range of hydrologic processes in this landscape, showcasing the importance of accurate geologic mapping and additional consideration of lithology in hazard mapping, water quality monitoring, or ecosystem assessments. For example, higher flooding risks may exist in downstream reaches of catchments with mélange bedrock or other shallow and low hydraulic conductivity bedrock, demonstrated by the flashier hydrology and significantly higher streamflow peaks observed at NDC. Further, catchments with shallow hydrologic flow paths can consistently mobilize higher concentrations of biogenic solutes (e.g., DOC, nitrogen, and phosphorus), which may influence in-stream biogeochemistry and downstream water quality. Further, extended periods of zero flow and sparse groundwater seeps in dry months in NDC suggest limited groundwater availability, creating highly restricted surface water refugia with implications for aquatic, riparian, and plant community health during periods of extended drought.

Data Availability Statement

All data used in the publication are available on the CUAHSI HydroShare data server (Giggy & Zimmer, 2025).

Acknowledgments

The authors would like to acknowledge the financial support provided by the National Science Foundation CAREER Grant (Award 2046957) and the Mildred E. Mathias Graduate Student Research Grant by the University of California Natural Reserve System. The authors would also like to acknowledge the financial support granted by the University of California Santa Cruz, through the Earth's Environment Award. We thank Dr. Mong-Han Huang for allowing us to add the seismic refraction survey results and assistance with adding descriptions of the data to the Supplemental Information. The authors thank Riley Barton and Dr. Sasha Wagner at Rensselaer Polytechnic Institute for contributing to our DOC sample analysis. The authors thank Dan Sampson and Brecky Morris for instrumentation design and troubleshooting. The authors are grateful for the support in the field and lab from past and present UC Santa Cruz Watershed Hydrology Lab members, particularly Peter Willits, Nerissa Barling, Michael Wilshire, and Dr. Amanda Donaldson. Further, the authors thank Zac Harlow and Zac Tuthill at BORR for land access and consistent fieldwork support.

References

Aitkenhead, J. A., Hope, D., & Billett, M. F. (1999). The relationship between dissolved organic carbon in stream water and soil organic carbon pools at different spatial scales. *Hydrological Processes*, *13*(8), 1289–1302. https://doi.org/10.1002/(SICI)1099-1085(19990615)13:8<1289::AID-HYP766>3.0.CO;2-M

Ameli, A. A., Beven, K., Erlandsson, M., Creed, I. F., McDonnell, J. J., & Bishop, K. (2016). Primary weathering rates, water transit times, and concentration-discharge relations: A theoretical analysis for the critical zone. *Water Resources Research*, *53*(1), 942–960. https://doi.org/10.1002/2016WR019448

Ameli, A. A., Laudon, H., Teutschbein, C., & Bishop, K. (2021). Where and when to collect tracer data to diagnose hillslope permeability architecture. *Water Resources Research*, *57*(8), e2020WR028719. https://doi.org/10.1029/2020WR028719

Anderson, S. P., Dietrich, W. E., Torres, R., Montgomery, D. R., & Loague, K. (1997). Concentration-discharge relationships in runoff from a steep, unchanneled catchment. *Water Resources Research*, *33*(1), 211–225. https://doi.org/10.1029/96WR02715

Aulenbach, B. T., Burns, D. A., Shanley, J. B., Yanai, R. D., Bae, K., Wild, A. D., et al. (2016). Approaches to stream solute load estimation for solutes with varying dynamics from five diverse small watersheds. *Ecosphere*, *7*(6), e01298. https://doi.org/10.1002/ecs2.1298

Bergstrom, A., Jencso, K., & McGlynn, B. (2016). Spatiotemporal processes that contribute to hydrologic exchange between hillslopes, valley bottoms, and streams. *Water Resources Research*, *52*(6), 4628–4645. https://doi.org/10.1002/2015WR017972

Bernal, S., Butturini, A., & Sabater, F. (2002). Variability of DOC and nitrate responses to storms in a small Mediterranean forested catchment. *Hydrology and Earth System Sciences*, *6*(6), 1031–1041. https://doi.org/10.5194/hess-6-1031-2002

Bernal, S., von Schiller, D., Sabater, F., & Martí, E. (2013). Hydrological extremes modulate nutrient dynamics in mediterranean climate streams across different spatial scales. *Hydrobiologia*, *719*(1), 31–42. https://doi.org/10.1007/s10750-012-1246-2

Beven, K. J., & Kirkby, M. J. (1979). A physically based, variable contributing area model of basin hydrology/Un modèle à base physique de zone d'appel variable de l'hydrologie du bassin versant. *Hydrological Sciences Bulletin*, *24*(1), 43–69. https://doi.org/10.1080/02626667909491834

Bieroza, M. Z., Heathwaite, A. L., Bechmann, M., Kyllmar, K., & Jordan, P. (2018). The concentration-discharge slope as a tool for water quality management. *Science of the Total Environment*, *630*, 738–749. https://doi.org/10.1016/j.scitotenv.2018.02.256

Bowering, K. L., Edwards, K. A., Prestegaard, K., Zhu, X., & Ziegler, S. E. (2020). Dissolved organic carbon mobilized from organic horizons of mature and harvested black spruce plots in a mesic boreal region. *Biogeosciences*, *17*(3), 581–595. https://doi.org/10.5194/bg-17-581-2020

Buttle, J. M. (1994). Isotope hydrograph separations and rapid delivery of pre-event water from drainage basins. *Progress in Physical Geography: Earth and Environment*, *18*(1), 16–41. https://doi.org/10.1177/030913339401800102

Callahan, R. P., Huang, M.-H., Donaldson, A., Hudson-Rasmussen, B., & Zimmer, M. (2024). Geologic and tectonic controls on deep fracturing, weathering, and water flow in the central California coast range. *Geophysical Research Letters*, *51*(13), e2024GL109129. https://doi.org/10.1029/2024GL109129

Carlton, C. W. (1963). *Drainage density and streamflow (geological survey professional paper 422–C)*. U.S. Department of the Interior, U.S. Geological Survey.

Cartwright, I., Morgenstern, U., & Hofmann, H. (2020). Concentration versus streamflow trends of major ions and tritium in headwater streams as indicators of changing water stores. *Hydrological Processes*, *34*(2), 485–505. https://doi.org/10.1002/hyp.13600

Chaussard, E., Bürgmann, R., Fattahi, H., Johnson, C. W., Nadeau, R., Taira, T., & Johanson, I. (2015). Interseismic coupling and refined earthquake potential on the Hayward-Calaveras fault zone. *Journal of Geophysical Research: Solid Earth*, *120*(12), 8570–8590. https://doi.org/10.1002/2015JB012230

Chorover, J., Derry, L. A., & McDowell, W. H. (2017). Concentration-discharge relations in the critical zone: Implications for resolving critical zone structure, function, and evolution. *Water Resources Research*, *53*(11), 8654–8659. https://doi.org/10.1002/2017WR021111

Clow, D. W., & Mast, M. A. (2010). Mechanisms for chemostatic behavior in catchments: Implications for CO2 consumption by mineral weathering. *Chemical Geology*, *269*(1–2), 40–51. https://doi.org/10.1016/j.chemgeo.2009.09.014

Conrad, O., Bechtel, B., Bock, M., Dietrich, H., Fischer, E., Gerlitz, L., et al. (2015). System for Automated Geoscientific Analyses (SAGA) v. 2.1.4 [Preprint]. *Climate and Earth System Modeling*. https://doi.org/10.5194/gmdd-8-2271-2015

Creed, I. F., McKnight, D. M., Pellerin, B. A., Green, M. B., Bergamaschi, B. A., Aiken, G. R., et al. (2015). The river as a chemostat: Fresh perspectives on dissolved organic matter flowing down the river continuum. *Canadian Journal of Fisheries and Aquatic Sciences*, *72*(8), 1272–1285. https://doi.org/10.1139/cjfas-2014-0400

Crowther, T. W., Van Den Hoogen, J., Wan, J., Mayes, M. A., Keiser, A. D., Mo, L., et al. (2019). The global soil community and its influence on biogeochemistry. *Science*, *365*(6455), eaav0550. https://doi.org/10.1126/science.aav0550

D'Amario, S. C., Wilson, H. F., & Xenopoulos, M. A. (2021). Concentration-discharge relationships derived from a larger regional dataset as a tool for watershed management. *Ecological Applications*, *31*(8), e02447. https://doi.org/10.1002/eap.2447

Day, T. J. (1976). On the precision of salt dilution gauging. *Journal of Hydrology*, *31*(3–4), 293–306. https://doi.org/10.1016/0022-1694(76)90130-x

Dettinger, M. D., Ralph, F. M., Das, T., Neiman, P. J., & Cayan, D. R. (2011). Atmospheric rivers, floods and the water resources of California. *Water*, *3*(2), 445–478. https://doi.org/10.3390/w3020445

Dibblee, T. W., & Munich, J. A. (2006). *Geologic map of the mount day quadrangle*. Santa Clara and Alameda Counties, California [Geologic Map]. Dibblee Geological Foundation.

Donaldson, A. M., Zimmer, M., Huang, M.-H., Johnson, K. N., Hudson-Rasmussen, B., Finnegan, N., et al. (2023). Symmetry in hillslope steepness and saprolite thickness between hillslopes with opposing aspects. *Journal of Geophysical Research: Earth Surface*, *128*(7), e2023JF007076. https://doi.org/10.1029/2023JF007076

Dosskey, M. G., & Bertsch, P. M. (1994). Forest sources and pathways of organic matter transport to a blackwater stream: A hydrologic approach. *Biogeochemistry*, *24*(1), 1–19. https://doi.org/10.1007/BF00001304

Dralle, D. N., Hahm, W. J., Rempe, D. M., Karst, N. J., Thompson, S. E., & Dietrich, W. E. (2018). Quantification of the seasonal hillslope water storage that does not drive streamflow: Catchment storage that does not drive streamflow. *Hydrological Processes*, *32*(13), 1978–1992. https://doi.org/10.1002/hyp.11627

Dralle, D. N., Rossi, G., Georgakakos, P., Hahm, W. J., Rempe, D. M., Blanchard, M., et al. (2023). The salmonid and the subsurface: Hillslope storage capacity determines the quality and distribution of fish habitat. *Ecosphere*, *14*(2), e4436. https://doi.org/10.1002/ecs2.4436

Ehrhardt, A., Berger, K., Filipović, V., Wöhling, T., Vogel, H.-J., & Gerke, H. H. (2022). Tracing lateral subsurface flow in layered soils by undisturbed monolith sampling, targeted laboratory experiments, and model-based analysis. *Vadose Zone Journal*, *21*(4), e20206. https://doi.org/10.1002/vzj2.20206

Eidenshink, J., Schwind, B., Brewer, K., Zhu, Z.-L., Quayle, B., & Howard, S. (2007). A project for monitoring trends in burn severity. *Fire Ecology*, *3*(1), 3–21. Article 1. https://doi.org/10.4996/fireecology.0301003

Fiebig, D. M., Lock, M. A., & Neal, C. (1990). Soil water in the riparian zone as a source of carbon for a headwater stream. *Journal of Hydrology*, *116*(1), 217–237. https://doi.org/10.1016/0022-1694(90)90124-G

Giani, G., Tarasova, L., Woods, R. A., & Rico-Ramirez, M. A. (2022). An objective time-series-analysis method for rainfall-runoff event identification. *Water Resources Research*, *58*(2), e2021WR031283. https://doi.org/10.1029/2021WR031283

Giggy, L., & Zimmer, M. (2025). The role of lithology on concentration-discharge relationships and carbon export in two adjacent headwater catchments [Dataset]. *HydroShare*. http://www.hydroshare.org/resource/fffd8a7330ba46c1b8011a3b07b279e7

Gnann, S. J., Coxon, G., Woods, R. A., Howden, N. J., & McMillan, H. K. (2021). Tossh: A toolbox for streamflow signatures in hydrology. *Environmental Modelling and Software*, *138*, 104983. https://doi.org/10.1016/j.envsoft.2021.104983

Godsey, S. E., Hartmann, J., & Kirchner, J. W. (2019). Catchment chemostasis revisited: Water quality responds differently to variations in weather and climate. *Hydrological Processes*, *33*(24), 3056–3069. https://doi.org/10.1002/hyp.13554

Godsey, S. E., Kirchner, J. W., & Clow, D. W. (2009). Concentration-discharge relationships reflect chemostatic characteristics of US catchments. *Hydrological Processes*, *23*(13), 1844–1864. https://doi.org/10.1002/hyp.7315

Grande, E., Zimmer, M. A., & Mallard, J. M. (2022). Storage variability controls seasonal runoff generation in catchments at the threshold between energy and water limitation. *Hydrological Processes*, *36*(10), e14697. https://doi.org/10.1002/hyp.14697

Gregory, K. J., & Walling, D. E. (1968). The variation of drainage density within a catchment. *International Association of Scientific Hydrology. Bulletin*, *13*(2), 61–68. https://doi.org/10.1080/02626666809493583

Gutiérrez-Jurado, K. Y., Partington, D., Batelaan, O., Cook, P., & Shanafield, M. (2019). What triggers streamflow for intermittent rivers and ephemeral streams in low-gradient catchments in mediterranean climates. *Water Resources Research*, *55*(11), 9926–9946. https://doi.org/10.1029/2019WR025041

Hahm, W. J., Rempe, D. M., Dralle, D. N., Dawson, T. E., Lovill, S. M., Bryk, A. B., et al. (2019). Lithologically controlled subsurface critical zone thickness and water storage capacity determine regional plant community composition. *Water Resources Research*, *55*(4), 3028–3055. https://doi.org/10.1029/2018WR023760

Hall, F. R. (1970). Dissolved solids-discharge relationships: 1. Mixing models. *Water Resources Research*, *6*(3), 845–850. https://doi.org/10.1029/WR006i003p00845

Han, X., Liu, J., Srivastava, P., Mitra, S., & He, R. (2020). Effects of critical zone structure on patterns of flow connectivity induced by rainstorms in a steep forested catchment. *Journal of Hydrology*, *587*, 125032. https://doi.org/10.1016/j.jhydrol.2020.125032

Heller, K., & Kleber, A. (2016). Hillslope runoff generation influenced by layered subsurface in a headwater catchment in Ore Mountains, Germany. *Environmental Earth Sciences*, *75*(11), 943. https://doi.org/10.1007/s12665-016-5750-y

Herndon, E. M., Dere, A. L., Sullivan, P. L., Norris, D., Reynolds, B., & Brantley, S. L. (2015). Landscape heterogeneity drives contrasting concentration–discharge relationships in shale headwater catchments. *Hydrology and Earth System Sciences*, *19*(8), 3333–3347. https://doi.org/10.5194/hess-19-3333-2015

Herschy, R. (1993). The velocity-area method. *Flow Measurement and Instrumentation*, *4*(1), 7–10. https://doi.org/10.1016/0955-5986(93)90004-3

Holz, G. K. (2010). Sources and processes of contaminant loss from an intensively grazed catchment inferred from patterns in discharge and concentration of thirteen analytes using high intensity sampling. *Journal of Hydrology*, *383*(3), 194–208. https://doi.org/10.1016/j.jhydrol.2009.12.036

Inamdar, S., Finger, N., Singh, S., Mitchell, M., Levia, D., Bais, H., et al. (2012). Dissolved organic matter (DOM) concentration and quality in a forested mid-Atlantic watershed, USA. *Biogeochemistry*, *108*(1–3), 55–76. https://doi.org/10.1007/s10533-011-9572-4

Jefferson, A., Grant, G. e., Lewis, S. l., & Lancaster, S. t. (2010). Coevolution of hydrology and topography on a basalt landscape in the Oregon Cascade Range, USA. *Earth Surface Processes and Landforms*, *35*(7), 803–816. https://doi.org/10.1002/esp.1976

Jennings, C. W., Gutierrez, C., Bryant, W., Saucedo, G., & Wills, C. (2010). *Geologic map of California [geologic data map GDM-2]*. California Geological Survey. Retrieved from https://maps.conservation.ca.gov/cgs/metadata/GDM_002_GMC_750k_v2_metadata.html

Jobbágy, E. G., & Jackson, R. B. (2000). The vertical distribution of soil organic carbon and its relation to climate and vegetation. *Ecological Applications*, *10*(2), 423–436. https://doi.org/10.1890/1051-0761(2000)010[0423:TVDOSO]2.0.CO;2

Kim, H., Dietrich, W. E., Thurnhoffer, B. M., Bishop, J. K. B., & Fung, I. Y. (2017). Controls on solute concentration-discharge relationships revealed by simultaneous hydrochemistry observations of hillslope runoff and stream flow: The importance of critical zone structure. *Water Resources Research*, *53*(2), 1424–1443. https://doi.org/10.1002/2016WR019722

Kirchner, J. W. (2009). Catchments as simple dynamical systems: Catchment characterization, rainfall-runoff modeling, and doing hydrology backward. *Water Resources Research*, *45*(2). https://doi.org/10.1029/2008WR006912

Klaus, J., & McDonnell, J. J. (2013). Hydrograph separation using stable isotopes: Review and evaluation. *Journal of Hydrology*, *505*, 47–64. https://doi.org/10.1016/j.jhydrol.2013.09.006

Knapp, J. L. A., & Musolff, A. (2024). Concentration-discharge relationships revisited: Overused but underutilised? *Hydrological Processes*, *38*(11), e15328. https://doi.org/10.1002/hyp.15328

Knapp, J. L. A., von Freyberg, J., Studer, B., Kiewiet, L., & Kirchner, J. W. (2020). Concentration–discharge relationships vary among hydrological events, reflecting differences in event characteristics. *Hydrology and Earth System Sciences*, *24*(5), 2561–2576. https://doi.org/10.5194/hess-24-2561-2020

Lapides, D. A., Hahm, W. J., Rempe, D. M., Dietrich, W. E., & Dralle, D. N. (2022). Controls on stream water age in a saturation overland flow-dominated catchment. *Water Resources Research*, *58*(4), e2021WR031665. https://doi.org/10.1029/2021WR031665

Li, H., & Ameli, A. A. (2023). Upland hillslope groundwater subsidy affects low-flow storage–discharge relationship. *Water Resources Research*, *59*(10), e2022WR034155. https://doi.org/10.1029/2022WR034155

Li, L., Bao, C., Sullivan, P. L., Brantley, S., Shi, Y., & Duffy, C. (2017). Understanding watershed hydrogeochemistry: 2. Synchronized hydrological and geochemical processes drive stream chemostatic behavior: Concentration-discharge relationship. *Water Resources Research*, *53*(3), 2346–2367. https://doi.org/10.1002/2016WR018935

Lindberg, S. E., Lovett, G. M., Richter, D. D., & Johnson, D. W. (1986). Atmospheric deposition and canopy interactions of major ions in a forest. *Science*, *231*(4734), 141–145. https://doi.org/10.1126/science.231.4734.141

Litwin, D. G., Tucker, G. E., Barnhart, K. R., & Harman, C. J. (2024). Catchmentcoevolution and the geomorphic origins ofvariable source area hydrology. *WaterResources Research*, *60*(6), e2023WR034647. https://doi.org/10.1029/2023WR034647

Lovill, S. M., Hahm, W. J., & Dietrich, W. E. (2018). Drainage from the critical zone: Lithologic controls on the persistence and spatial extent of wetted channels during the summer dry season. *Water Resources Research*, *54*(8), 5702–5726. https://doi.org/10.1029/2017WR021903

Luo, W., Jasiewicz, J., Stepinski, T., Wang, J., Xu, C., & Cang, X. (2016). Spatial association between dissection density and environmental factors over the entire conterminous United States. *Geophysical Research Letters*, *43*(2), 692–700. https://doi.org/10.1002/2015GL066941

Maher, K. (2010). The dependence of chemical weathering rates on fluid residence time. *Earth and Planetary Science Letters*, *294*(1–2), 101–110. https://doi.org/10.1016/j.epsl.2010.03.010

Maher, K. (2011). The role of fluid residence time and topographic scales in determining chemical fluxes from landscapes. *Earth and Planetary Science Letters*, *312*(1–2), 48–58. https://doi.org/10.1016/j.epsl.2011.09.040

McMillan, H., Coxon, G., Araki, R., Salwey, S., Kelleher, C., Zheng, Y., et al. (2023). When good signatures go bad: Applying hydrologic signatures in large sample studies. *Hydrological Processes*, *37*(9), 14987. https://doi.org/10.1002/hyp.14987

Moatar, F., Abbott, B. W., Minaudo, C., Curie, F., & Pinay, G. (2017). Elemental properties, hydrology, and biology interact to shape concentration-discharge curves for carbon, nutrients, sediment, and major ions. *Water Resources Research*, *53*(2), 1270–1287. https://doi.org/10.1002/2016WR019635

Mulholland, P. J. (1993). Hydrometric and stream chemistry evidence of three storm flowpaths in Walker Branch Watershed. *Journal of Hydrology*, *151*(2), 291–316. https://doi.org/10.1016/0022-1694(93)90240-A

Musolff, A., Fleckenstein, J. H., Rao, P. S. C., & Jawitz, J. W. (2017). Emergent archetype patterns of coupled hydrologic and biogeochemical responses in catchments. *Geophysical Research Letters*, *44*(9), 4143–4151. https://doi.org/10.1002/2017GL072630

Nippgen, F., McGlynn, B. L., Marshall, L. A., & Emanuel, R. E. (2011). Landscape structure and climate influences on hydrologic response: Landscape and climate influences on hydrology. *Water Resources Research*, *47*(12). https://doi.org/10.1029/2011WR011161

Page, B. M. (1999). Geology of the lick observatory Quadrangle, California. *International Geology Review*, *41*(4), 355–367. https://doi.org/10.1080/00206819909465146

Patton, P. C., & Baker, V. R. (1976). Morphometry and floods in small drainage basins subject to diverse hydrogeomorphic controls. *Water Resources Research*, *12*(5), 941–952. https://doi.org/10.1029/WR012i005p00941

Pfister, L., Martínez-Carreras, N., Hissler, C., Klaus, J., Carrer, G. E., Stewart, M. K., & McDonnell, J. J. (2017). Bedrock geology controls on catchment storage, mixing, and release: A comparative analysis of 16 nested catchments. *Hydrological Processes*, *31*(10), 1828–1845. https://doi.org/10.1002/hyp.11134

Ploum, S. W., Laudon, H., Peralta-Tapia, A., & Kuglerová, L. L. (2020). Are dissolved organic carbon concentrations in riparian groundwater linked to hydrological pathways in the boreal forest? *Hydrology and Earth System Sciences*, *24*(4), 1709–1720. https://doi.org/10.5194/hess-24-1709-2020

Prancevic, J. P., & Kirchner, J. W. (2019). Topographic controls on the extension and retraction of flowing streams. *Geophysical Research Letters*, *46*(4), 2084–2092. https://doi.org/10.1029/2018GL081799

Raymond, L. A. (2018). What is Franciscan? Revisited. *International Geology Review*, *60*(16), 1968–2030. https://doi.org/10.1080/00206814.2017.1396933

Raymond, P. A., & Saiers, J. E. (2010). Event controlled DOC export from forested watersheds. *Biogeochemistry*, *100*(1), 197–209. https://doi.org/10.1007/s10533-010-9416-7

Rempe, D. M., & Dietrich, W. E. (2018). Direct observations of rock moisture, a hidden component of the hydrologic cycle. *Proceedings of the National Academy of Sciences*, *115*(11), 2664–2669. https://doi.org/10.1073/pnas.1800141115

Rose, L. A., Karwan, D. L., & Godsey, S. E. (2018). Concentration–discharge relationships describe solute and sediment mobilization, reaction, and transport at event and longer timescales. *Hydrological Processes*, *32*(18), 2829–2844. https://doi.org/10.1002/hyp.13235

Salve, R., Rempe, D. M., & Dietrich, W. E. (2012). Rain, rock moisture dynamics, and the rapid response of perched groundwater in weathered, fractured argillite underlying a steep hillslope. *Water Resources Research*, *48*(11). https://doi.org/10.1029/2012WR012583

Sangireddy, H., Carothers, R. A., Stark, C. P., & Passalacqua, P. (2016). Controls of climate, topography, vegetation, and lithology on drainage density extracted from high resolution topography data. *Journal of Hydrology*, *537*, 271–282. https://doi.org/10.1016/j.jhydrol.2016.02.051

Schemmann, K., Unruh, J. R., & Moores, E. M. (2008). Kinematics of Franciscan complex exhumation: New insights from the geology of mount Diablo, California. *GSA Bulletin*, *120*(5–6), 543–555. https://doi.org/10.1130/B26056.1

Sklash, M. G., & Farvolden, R. N. (1979). The role of groundwater in storm runoff. *Journal of Hydrology, The George Burke Maxey Memorial*, (43), 45–65. https://doi.org/10.1016/s0167-5648(09)70009-7

Sklash, M. G., Farvolden, R. N., & Fritz, P. (1976). A conceptual model of watershed response to rainfall, developed through the use of oxygen-18 as a natural tracer. *Canadian Journal of Earth Sciences*, *13*(2), 271–283. https://doi.org/10.1139/e76-029

Speir, S. L., Rose, L. A., Blaszczak, J. R., Kincaid, D. W., Fazekas, H. M., Webster, A. J., et al. (2024). Catchment concentration–discharge relationships across temporal scales: A review. *WIREs Water*, *11*(2), e1702. https://doi.org/10.1002/wat2.1702

Stewart, B., Shanley, J. B., Kirchner, J. W., Norris, D., Adler, T., Bristol, C., et al. (2022). Streams as mirrors: Reading subsurface water chemistry from stream chemistry. *Water Resources Research*, *58*(1), e2021WR029931. https://doi.org/10.1029/2021WR029931

Strohmeier, S., Knorr, K.-H., Reichert, M., Frei, S., Fleckenstein, J. H., Peiffer, S., & Matzner, E. (2012). Concentrations and fluxes of dissolved organic carbon in runoff from a forested catchment: Insights from high frequency measurements [Preprint]. *Biogeochemistry: Rivers and Streams*. https://doi.org/10.5194/bgd-9-11925-2012

Tague, C., & Grant, G. E. (2004). A geological framework for interpreting the low-flow regimes of Cascade streams, Willamette River Basin, Oregon. *Water Resources Research*, *40*(4). https://doi.org/10.1029/2003WR002629

Uzun, H., Dahlgren, R. A., Olivares, C., Erdem, C. U., Karanfil, T., & Chow, A. T. (2020). Two years of post-wildfire impacts on dissolved organic matter, nitrogen, and precursors of disinfection by-products in California stream waters. *Water Research*, *181*, 115891. https://doi.org/10.1016/j.watres.2020.115891

van Meerveld, H. J. I., Peters, N. E., & McDonnell, J. J. (2007). Effect of bedrock permeability on subsurface stormflow and the water balance of a trenched hillslope at the Panola Mountain Research Watershed, Georgia, USA. *Hydrological Processes*, *21*(6), 750–769. https://doi.org/10.1002/hyp.6265

Vázquez, E., Romaní, A. M., Sabater, F., & Butturini, A. (2007). Effects of the dry–wet hydrological shift on dissolved organic carbon dynamics and fate across stream–riparian interface in a mediterranean catchment. *Ecosystems*, *10*(2), 239–251. https://doi.org/10.1007/s10021-007-9016-0

von Freyberg, J., Studer, B., Rinderer, M., & Kirchner, J. W. (2018). Studying catchment storm response using event- and pre-event-water volumes as fractions of precipitation rather than discharge. *Hydrology and Earth System Sciences*, *22*(11), 5847–5865. https://doi.org/10.5194/hess-22-5847-2018

Wakabayashi, J. (2017). Structural context and variation of ocean plate stratigraphy, Franciscan Complex, California: Insight into mélange origins and subduction-accretion processes. *Progress in Earth and Planetary Science*, *4*(1), 18. https://doi.org/10.1186/s40645-017-0132-y

Wei, X., Hayes, D. J., & Fernandez, I. (2021). Fire reduces riverine DOC concentration draining a watershed and alters post-fire DOC recovery patterns. *Environmental Research Letters*, *16*(2), 024022. https://doi.org/10.1088/1748-9326/abd7ae

Wentworth, C. M., Blake, M. C., McLaughlin, R. J., & Graymer, R. W. (1999). *Preliminary geologic map of the San Jose 30 X 60-minute quadrangle*. U.S. Geological Survey. California [Geologic Map].

Wu, Y., Su, H., Cheng, L., Qin, S., Zou, K., Liu, Y., et al. (2024). Exploring hydrological controls on dissolved organic carbon export dynamics in a typical flash flood catchment using a process-based model. *Science of the Total Environment*, *921*, 171139. https://doi.org/10.1016/j.scitotenv.2024.171139

Xiao, D., Shi, Y., Brantley, S. L., Forsythe, B., DiBiase, R., Davis, K., & Li, L. (2019). Streamflow generation from catchments of contrasting lithologies: The role of soil properties, topography, and catchment size. *Water Resources Research*, *55*(11), 9234–9257. https://doi.org/10.1029/2018WR023736

Xiao, H. B., Zhou, C., Hu, X. D., Wang, J., Wang, L., Huang, J. Q., et al. (2024). Subsurface hydrological connectivity controls nitrate export flux in a hilly catchment. *Water Research*, *253*, 121308. https://doi.org/10.1016/j.watres.2024.121308

Yoshida, T., & Troch, P. A. (2016). Coevolution of volcanic catchments in Japan. *Hydrology and Earth System Sciences*, *20*(3), 1133–1150. https://doi.org/10.5194/hess-20-1133-2016

Zarnetske, J. P., Bouda, M., Abbott, B. W., Saiers, J., & Raymond, P. A. (2018). Generality of hydrologic transport limitation of watershed organic carbon flux across ecoregions of the United States. *Geophysical Research Letters*, *45*(21). https://doi.org/10.1029/2018GL080005

Zhi, W., & Li, L. (2020). The shallow and deep hypothesis: Subsurface vertical chemical contrasts shape nitrate export patterns from different land uses. *Environmental Science and Technology*, *54*(19), 11915–11928. https://doi.org/10.1021/acs.est.0c01340

Zimmer, M. A., & McGlynn, B. L. (2018). Lateral, vertical, and longitudinal source area connectivity drive runoff and carbon export across watershed scales. *Water Resources Research*, *54*(3), 1576–1598. https://doi.org/10.1002/2017WR021718